

Goodness-of-fit tests for heavy-tailed random fields

Ying Niu,¹ Zhao Chen,² Christina Dan Wang³ and Yuwei Zhao^{4,*}

¹Shanghai Center for Mathematical Sciences, Fudan University, 220 Handan Road, CN-200433, Shanghai, China, ²School of Data Science, Fudan University, 220 Handan Road, CN-200433, Shanghai, China, ³Business Division, New York University Shanghai, 567 West Yangsi Road, CN-200124, Shanghai, China and ⁴Department of Foundational Mathematics, Xi'an Jiaotong-Liverpool University, 110 Ren'ai Road, CN-215123, Jiangsu, China

*Yuwei Zhao, Xi'an Jiaotong-Liverpool University, Suzhou, CN-215123, China. yuwei.zhao@xjtlu.edu.cn

FOR PUBLISHER ONLY Received on Date Month Year; revised on Date Month Year; accepted on Date Month Year

Abstract

We develop goodness-of-fit tests for max-stable random fields, which are used to model heavy-tailed spatial data. The test statistics are constructed based on the Fourier transforms of the indicators of extreme values in the heavy-tailed spatial data, whose asymptotic distribution is a Gaussian random field under a hypothesized max-stable random field. Since the covariance structure of the limiting Gaussian random field lacks an explicit expression, we propose a stationary bootstrap procedure for spatial fields to approximate critical values. Simulation studies confirm the theoretical distributional results, and applications to PM2.5 and temperature data illustrate the practical utility of the proposed method for model assessment.

Key words: Bootstrap, Fourier analysis, Goodness-of-fit test, Random field, Regular variation

1. Introduction

Heavy-tailed parametric models in Embrechts et al. (1997) provide a natural framework for modeling extremes in the time series setting. By far the most common of such models are max-stable models, including the max-moving averages and the Brown-Resnick model. These models are generalized for random fields, and they are widely used in analyzing the extremes of climate data, for instance, in temperature studies (Davison and Gholamrezaee, 2012; Oesting and Strokorb, 2022) and assessments of water levels (Huser and Davison, 2014; Asadi et al., 2015). Despite substantial progress in modeling extreme events, relatively little attention has been devoted to developing goodness-of-fit tests for these models. These tests are essential for validating distributional assumptions and ensuring reliable inferences.

Our goodness-of-fit tests are based on the dependence structure of extremes in a strictly stationary, isotropic, and heavy-tailed \mathbb{R}^d -valued random field $(X_{\mathbf{t}})_{\mathbf{t} \in \mathbb{Z}^2}$ with a generic element X , where d is a positive integer. Note that the field need not be Markovian. To our knowledge, goodness-of-fit tests for random fields are only developed for Markov random fields in Kaiser et al. (2012); Biswas et al. (2024). Instead of working with $X_{\mathbf{t}}$, we deal with its indicator of an extreme, $\mathbf{1}(|X_{\mathbf{t}}| > x)$. Here, $|\cdot|$ is the norm of X , x is a relatively large positive real number, the event $\{|X_{\mathbf{t}}| > x\}$ represents that an extreme happens at the location \mathbf{t} , and the indicator function $\mathbf{1}(\cdot)$ takes value 1 when the event happens and value 0 otherwise. With a proper normalizing parameter $(\mathbb{P}(|X| > x))^{-1}$, the limit of the covariance between $\mathbf{1}(|X_{\mathbf{t}}| > x)$ and $\mathbf{1}(|X_{\mathbf{t}+\mathbf{h}}| > x)$ for some $\mathbf{h} \in \mathbb{Z}^2$ as $x \rightarrow +\infty$ exists under mild conditions, and this limit is referred to as the *spatial extremogram* for $(X_{\mathbf{t}})$ in Cho et al. (2016). The Fourier transform and the inverse Fourier transform of the spatial extremogram are called the *extremal periodogram* and the *extremal integrated*

periodogram, respectively. The test statistic of the goodness-of-fit test is defined as a continuous function of the extremal integrated periodogram. We will prove a functional central limit theorem for the extremal integrated periodogram, whose limit is a Gaussian random field without an explicit expression of the covariance matrix, and the asymptotic distribution of the test statistic is obtained by an application of continuous mapping theorem. We will use numerical methods to derive the critical values for the test, including a Monte Carlo method and a bootstrap procedure. Our results extend the results on the spatial extremogram, the extremal periodogram, and the extremal integrated periodogram for a heavy-tailed time series in a series of papers by Mikosch et al. (Davis and Mikosch, 2009; Mikosch and Zhao, 2015, 2014; Davis et al., 2013a).

We assume that the random field $(X_{\mathbf{t}})$ is observed on an $n \times n$ lattice $\Lambda_n^2 = \{1, \dots, n\}^2$. Let $M_0 = M_0(\phi)$ represent a max-stable model with parameter $\phi \in \Phi$, where Φ is a compact parameter space. Our goal is to test whether $(X_{\mathbf{t}})_{\mathbf{t} \in \Lambda_n}$ follows the model M_0 . The hypotheses of the goodness-of-fit test are given by

- The null hypothesis H_0 : there exists $\phi \in \Phi$ such that $(X_{\mathbf{t}})_{\mathbf{t} \in \Lambda_n^2}$ comes from the max-stable model $M_0(\phi)$.
- The alternative hypothesis H_1 : Not H_0 .

Performing the goodness-of-fit test involves estimating the parameter(s) ϕ . The composite likelihood method for estimating ϕ has been extensively studied in Davison and Gholamrezaee (2012); Davis et al. (2013b,c); Asadi et al. (2015); Buhl et al. (2019). More recent advances include the Whittle estimator (Damek et al., 2023) on regular grids and the M-estimator (Einmahl et al., 2016) for irregularly

spaced spatial data. Both of these latter two methods will be employed in our numerical experiments, depending on the data structure.

Besides the classical Monte Carlo method, we develop a stationary bootstrap procedure to obtain the asymptotic distribution of the test statistic, from which the critical value for the goodness-of-fit test is calculated. The stationary bootstrap algorithm proposed by Politis and Romano (1994) is tailored for one-dimensional time series. A frequency-domain bootstrap method developed by Ng et al. (2021) involves resampling Fourier coefficients and an inverse transform, leading to relatively complex operations. To overcome these limitations, we introduce a two-dimensional stationary bootstrap procedure. By independently resampling blocks along rows and columns, our method preserves the spatial dependence structure of the original field. We will prove that the bootstrapped test statistic shares the same asymptotic distribution as the original test statistic.

The rest of the paper is organized as follows. Section 2 describes the test statistic and the procedure of performing the goodness-of-fit test. The asymptotic property of the test statistic is studied in Section 3. Section 4 provides a bootstrap procedure for the goodness-of-fit test, and the asymptotic properties of the bootstrapped test statistic are discussed. The distributional results are verified through simulations in Section 5. Finally, we take two applications as examples to illustrate the method for model assessment in Section 6. The Online Supplementary Material (Niu et al., 2025b) collects all the proofs.

2. Methodology: the goodness-of-fit test

2.1. Fourier analysis of a regularly varying random field

We consider a strictly stationary and isotropic random field $(X_{\mathbf{t}})_{\mathbf{t} \in \mathbb{Z}^2}$ taking values from \mathbb{R}^d for some $d \geq 1$. We say that $(X_{\mathbf{t}})_{\mathbf{t} \in \mathbb{Z}^2}$ is *regularly varying with tail index* $\xi > 0$, if there exists a random field $(\Xi_{\mathbf{t}})_{\mathbf{t} \in \mathbb{Z}^2}$ and some $\xi > 0$ such that for any finite subset $A \subset \mathbb{Z}^2$ and $t > 0$,

$$\mathbb{P}((X_{\mathbf{t}}/|X_{\mathbf{0}}|)_{\mathbf{t} \in A} \in \cdot \mid |X_{\mathbf{0}}| > x) \xrightarrow{w} \mathbb{P}((\Xi_{\mathbf{t}})_{\mathbf{t} \in A} \in \cdot), \quad (1)$$

$$\frac{\mathbb{P}(|X| > tx)}{\mathbb{P}(|X| > x)} \rightarrow t^{-\xi}, \quad x \rightarrow \infty. \quad (2)$$

Here, \xrightarrow{w} denotes weak convergence of probability measures.

Regular variation captures the heavy-tailed characteristic of the data and serves as an important condition for quantifying extremal dependence; see Basrak and Segers (2009); Segers et al. (2017); Wu and Samorodnitsky (2020); Basrak and Planinić (2021). According to Cho et al. (2016), the *spatial extremogram* for $(X_{\mathbf{t}})_{\mathbf{t} \in \mathbb{Z}^2}$ is given by

$$\begin{aligned} \gamma(\mathbf{h}) &= \gamma(h_1, h_2) = \lim_{x \rightarrow \infty} \mathbb{P}(|X_{\mathbf{h}}| > x \mid |X_{\mathbf{0}}| > x) \\ &= \lim_{x \rightarrow \infty} \text{corr}(\mathbf{1}(|X_{\mathbf{h}}| > x), \mathbf{1}(|X_{\mathbf{0}}| > x)) = \mathbb{E}[1 \wedge |\Xi_{\mathbf{h}}|^\xi]. \end{aligned}$$

Here $|\cdot|$ is the norm in \mathbb{R}^d and $\mathbf{1}(\cdot)$ is the indicator function. It generalizes the extremogram for time series in Davis and Mikosch (2009) to spatial settings and captures the “autocorrelation” of extreme events in a random field. The isotropic property implies that $\gamma(\mathbf{h}) = \gamma(\|\mathbf{h}\|)$.

If

$$\sum_{\mathbf{h} \in \mathbb{Z}^2} |\gamma(\mathbf{h})| < \infty, \quad (3)$$

the Fourier transform of $(\gamma(\mathbf{h}))$,

$$f(\boldsymbol{\omega}) = \sum_{\mathbf{h} \in \mathbb{Z}^2} \gamma(\mathbf{h}) \exp\{-i\mathbf{h}^\top \boldsymbol{\omega}\} = \sum_{\mathbf{h} \in \mathbb{Z}^2} \gamma(\mathbf{h}) \cos(\mathbf{h}^\top \boldsymbol{\omega}), \quad \boldsymbol{\omega} \in [0, 2\pi]^2 =: \Pi^2 \quad (4)$$

exists. Due to the isotropic property, the imaginary part of $f(\boldsymbol{\omega})$ vanishes. The function $f(\boldsymbol{\omega})$ is called the *extremal spectral density* for $(X_{\mathbf{t}})_{\mathbf{t} \in \mathbb{Z}^2}$. A natural estimator for $f(\boldsymbol{\omega})$ is the *extremal periodogram*,

$$\tilde{f}(\boldsymbol{\omega}) = \sum_{\|\mathbf{h}\| < n} \tilde{\gamma}(\mathbf{h}) \cos(\mathbf{h}^\top \boldsymbol{\omega}),$$

where $\tilde{\gamma}(\mathbf{h}) = (m_n/n^2) \sum_{\mathbf{t}, \mathbf{t}+\mathbf{h} \in \Lambda_n^2} \tilde{I}_{\mathbf{t}} \tilde{I}_{\mathbf{t}+\mathbf{h}}$, with $\tilde{I}_{\mathbf{t}} = I_{\mathbf{t}} - p_n(\mathbf{0})$, $I_{\mathbf{t}} = \mathbf{1}(|X_{\mathbf{t}}| > a_{m_n})$ and $p_n(\mathbf{h}) = \mathbb{P}(\min(|X_{\mathbf{0}}|, |X_{\mathbf{h}}|) > a_{m_n})$. Here, (m_n) is a sequence of positive integers satisfying $m_n \rightarrow \infty$ and $m_n/n \rightarrow 0$ as $n \rightarrow \infty$. The sequence (a_{m_n}) is chosen as the $(1 - 1/m_n)$ -th quantile of $|X|$, i.e., $\mathbb{P}(|X| > a_{m_n}) = 1/m_n$.

2.2. Test statistic and the test procedure

We consider the inverse Fourier transform of $(\gamma(\mathbf{h}))$, the *extremal integrated spectral density* (with respect to a function $g : \Pi^2 \rightarrow \mathbb{R}_+$),

$$J(\boldsymbol{\omega}; g) = J(\boldsymbol{\omega}) = \int_{[0, \omega_1] \times [0, \omega_2]} f(\mathbf{x}) g(\mathbf{x}) d\mathbf{x}, \quad \boldsymbol{\omega} = (\omega_1, \omega_2) \in \Pi^2.$$

The function g is Lipschitz continuous and L^2 -integrable over Π^2 . By replacing $f(\boldsymbol{\omega})$ with the right-hand side of (4), we have

$$J(\boldsymbol{\omega}) = \sum_{\mathbf{h} \in \mathbb{Z}^2} \gamma(h) \psi_{\mathbf{h}}(\boldsymbol{\omega}),$$

where $\psi_{\mathbf{h}}(\boldsymbol{\omega}) = \int_{[0, \omega_1] \times [0, \omega_2]} g(\mathbf{x}) \cos(\mathbf{h}^\top \mathbf{x}) d\mathbf{x}$. By discretizing the integral in $\psi_{\mathbf{h}}$, we have $\tilde{\psi}_{\mathbf{h}}(\boldsymbol{\omega}) = (4\pi^2/n^2) \sum_{i_1=1}^{j_1} \sum_{i_2=1}^{j_2} g(\boldsymbol{\lambda}_{\mathbf{i}}) \cos(\mathbf{h}^\top \boldsymbol{\lambda}_{\mathbf{i}})$ with $\boldsymbol{\lambda}_{\mathbf{i}} = (\lambda_{i_1}, \lambda_{i_2}) = (2\pi i_1/n, 2\pi i_2/n)$ for $1 \leq i_1, i_2 \leq n$ and $j_i = \lfloor n\omega_i/(2\pi) \rfloor$ is the integer part of $n\omega_i/(2\pi)$ for $i = 1, 2$. The *extremal integrated periodogram* $\tilde{J}_n(\boldsymbol{\omega})$ is given by $\tilde{J}_n(\boldsymbol{\omega}) = \sum_{\|\mathbf{h}\| < n} \tilde{\gamma}(\mathbf{h}) \tilde{\psi}_{\mathbf{h}}(\boldsymbol{\omega})$. We will prove that $\tilde{J}_n(\boldsymbol{\omega})$ multiplied by a proper normalizing parameter converges to a Gaussian random field in Section 3. We propose the *Grenander-Rosenblatt statistic* (GRS)

$$T_n = \frac{n}{\sqrt{m_n}} \sup_{\boldsymbol{\omega} \in \Pi^2} |\tilde{J}_n(\boldsymbol{\omega}) - \mathbb{E}[\tilde{J}_n(\boldsymbol{\omega})]| = \frac{n}{\sqrt{m_n}} \sup_{1 \leq i_1, i_2 \leq n} |\tilde{J}_n(\boldsymbol{\lambda}_{\mathbf{i}}) - \mathbb{E}[\tilde{J}_n(\boldsymbol{\lambda}_{\mathbf{i}})]|.$$

Other test statistics for testing the fit of a Gaussian sheet, such as the Cramér-von Mises statistic, can be defined in a similar way.

We propose a testing procedure based on the statistic T_n . Recall that the null hypothesis H_0 is that the observation $(X_{\mathbf{t}})_{\mathbf{t} \in \Lambda_n^2} = (X_{\mathbf{t}}^{(0)})_{\mathbf{t} \in \Lambda_n^2}$ comes from the max-stable model $M_0(\phi)$ with a parameter ϕ . Under the hypothesis H_0 , we estimate ϕ from the observation $(X_{\mathbf{t}})_{\mathbf{t} \in \Lambda_n^2}$ and the estimated value of ϕ is denoted by $\hat{\phi} = \hat{\phi}_n$. By using the Monte Carlo method, we can simulate B samples $(X_{\mathbf{t}}^{(b)})_{\mathbf{t} \in \Lambda_n^2, b=1, \dots, B}$ from the model $M_0(\hat{\phi})$. The quantity a_{m_n} with a pre-determined value m_n is the $(1 - 1/m_n)$ -th empirical quantile of $\{X_{\mathbf{t}}^{(b)}, b = 1, 2, \dots, B\}$, and we calculate $(I_{\mathbf{t}}^{(b)})_{\mathbf{t} \in \Lambda_n^2, b=0, 1, \dots, B} = (\mathbf{1}(|X_{\mathbf{t}}^{(b)}| > a_{m_n}))_{\mathbf{t} \in \Lambda_n^2, b=0, 1, \dots, B}$, $\tilde{\gamma}^{(B)}(\mathbf{h})$, and consequently,

$(\tilde{J}_n^{(b)}(\boldsymbol{\lambda}_i))$ for $b = 0, 1, \dots, B$ and $1 \leq i_1, i_2 \leq n$. The quantity $\mathbb{E}[\tilde{J}_n(\boldsymbol{\lambda}_i)]$ is obtained as the average of $(\tilde{J}_n^{(b)}(\boldsymbol{\lambda}_i))_{b=1, \dots, B}$ for all $1 \leq i_1, i_2 \leq n$. For $b = 0, 1, 2, \dots, B$, we replace $\tilde{J}_n(\boldsymbol{\omega})$ in the formula of T_n with $\tilde{J}_n^{(b)}(\boldsymbol{\omega})$, and obtain the *simulation-based statistic* $T_n(b)$. Let $\alpha \in (0, 1)$ be a pre-determined level of significance, and we choose the $(1 - \alpha)$ -th quantile of $\{T_n(b) : b = 1, 2, \dots, B\}$ as the critical value $c_n(\alpha)$ for the test. We reject the null hypothesis H_0 in favor of H_1 at the α -level of significance if $T_n(0) > c_n(\alpha)$; otherwise, we cannot reject H_0 . We refer to $c_n(\alpha)$ as the *simulation-based threshold* at the α -level of significance.

Another way to approximate the asymptotic distribution of T_n is to apply a bootstrap procedure developed in Section 4. By choosing the same a_{m_n} as above, we will generate the bootstrap samples $(X_{\mathbf{t}^\star}^{(b)})_{\mathbf{t} \in \Lambda_n^2; b=1, 2, \dots, B}$ from $(X_{\mathbf{t}})_{\mathbf{t} \in \Lambda_n^2} = (X_{\mathbf{t}^\star}^{(0)})_{\mathbf{t} \in \Lambda_n^2}$ to compute the *bootstrapped extremal integrated periodogram* $\hat{J}_n^\star(\boldsymbol{\omega})(b)$ for $b = 1, 2, \dots, B$. We assume that $\hat{J}_n^\star(\boldsymbol{\omega})(0)$ is calculated from the original observation $(X_{\mathbf{t}})_{\mathbf{t} \in \Lambda_n^2}$. Write the *bootstrap-based statistic* $T_n^\star(b) = (n/\sqrt{m_n}) \sup_{\boldsymbol{\omega} \in \Pi^2} |\hat{J}_n^\star(\boldsymbol{\omega})(b) - \mathbb{E}^\star[\hat{J}_n^\star(\boldsymbol{\omega})]|$ for $b = 0, 1, \dots, B$, where $\mathbb{E}^\star[\hat{J}_n^\star(\boldsymbol{\omega})] = B^{-1} \sum_{b=1}^B \hat{J}_n^\star(\boldsymbol{\omega})(b)$. Take $c_n^\star(\alpha)$ as the $(1 - \alpha)$ -quantile of $\{T_n^\star(b) : b = 1, \dots, B\}$. The asymptotic distributions of T_n and T_n^\star are the same. We reject H_0 in favor of H_1 at the α -level of significance if $T_n(0) > c_n^\star(\alpha)$; otherwise, we cannot reject H_0 . We refer to $c_n^\star(\alpha)$ as the *bootstrapped-based threshold* at the α -level of significance.

The choice of the value a_{m_n} plays a vital role in the procedure of the goodness-of-fit test, which is estimated under the null hypothesis. If the null hypothesis is false, the estimation of a_{m_n} is incorrect, and consequently both $\tilde{J}_n(\boldsymbol{\lambda}_i)$ and its centering $\mathbb{E}[\tilde{J}_n(\boldsymbol{\lambda}_i)]$ are incorrect. The errors would be magnified due to the mismatch between a_{m_n} and the normalizing parameter m_n . The quantities \tilde{J}_n and \hat{J}_n^\star are mainly determined by the extremal dependence structure of the embedded model M_0 . The

values of \tilde{J}_n and \tilde{J}_n^\star are not susceptible to the changes of ϕ , but they are sensitive to the change of the embedded model M_0 . Our proposed test statistic T_n is proper to test the fit of the model M_0 . We will examine the efficiency of the goodness-of-fit test through simulation studies in Section 5.

3. Asymptotic distribution of the test statistic

3.1. Mixing conditions

We introduce mixing conditions for deriving the functional central limit theorem for the extremal integrated periodogram $\tilde{J}_n(\omega)$. The α -mixing coefficient between two σ -fields \mathcal{A} and \mathcal{B} on a sample space Ω is given in Rosenblatt (1956) by $\alpha(\mathcal{A}, \mathcal{B}) = \sup_{A \in \mathcal{A}, B \in \mathcal{B}} |\mathbb{P}(A \cap B) - \mathbb{P}(A)\mathbb{P}(B)|$. For a random field $(X_{\mathbf{t}})_{\mathbf{t} \in \mathbb{Z}^2}$, Rosenblatt (1985) defined a specific α -mixing coefficient by $\alpha_{j,k}(h) = \sup_{S, T \subset \mathbb{Z}^2, \#S \leq j, \#T \leq k, \|S - T\| \geq h} \alpha(\sigma(X_{\mathbf{s}}, \mathbf{s} \in S), \sigma(X_{\mathbf{t}}, \mathbf{t} \in T))$, where $\sigma(X_{\mathbf{s}}, \mathbf{s} \in Q)$ denotes the σ -field generated by $\{X_{\mathbf{s}}, \mathbf{s} \in Q\}$ for $Q \subset \mathbb{Z}^2$.

Assumption 1 *Let $(X_{\mathbf{t}})_{\mathbf{t} \in \mathbb{Z}^2}$ be a strictly stationary and isotropic random field that is regularly varying with index $\xi > 0$ and α -mixing with coefficients $(\alpha_{j,k})$. Furthermore, there exist integer sequences (m_n) and (r_n) such that $m_n, r_n \rightarrow \infty$, $m_n/n \rightarrow 0$, $r_n^4/m_n \rightarrow 0$, $nr_n/m_n^{3/2} \rightarrow 0$, and the following conditions hold:*

(a) *For every $\delta > 0$,*

$$\lim_{h \rightarrow \infty} \limsup_{n \rightarrow \infty} m_n \sum_{\mathbf{h}: h < \|\mathbf{h}\| \leq r_n} \mathbb{P}(|X_{\mathbf{0}}| > \delta a_{m_n}, |X_{\mathbf{h}}| > \delta a_{m_n}) = 0. \quad (5)$$

(b) *There exist constants $K, \tau > 0$, $\rho \in (0, 1)$ and a non-increasing function $\alpha(h)$ such that $\sup_{j,k \geq 1} \alpha_{j,k}(h) \leq \alpha(h) \leq K\rho^{h^\tau}$ and $\lim_{n \rightarrow \infty} m_n \alpha(r_n) = 0$.*

Assumption 1 is pivotal for establishing asymptotic properties and aligns with the condition **(M1)** in Damek et al. (2023). Specially, Assumption 1(b) implies that

$$\lim_{n \rightarrow \infty} m_n \sum_{\|\mathbf{h}\| > r_n} \alpha(\|\mathbf{h}\|) = 0. \quad (6)$$

3.2. Asymptotic properties of the extremal integrated periodogram

We start with the unbiasedness of $\tilde{J}_n(\boldsymbol{\omega})$.

Theorem 1 *Suppose Assumption 1 holds. For all $\boldsymbol{\omega} \in \Pi^2$,*

$$\mathbb{E}[\tilde{J}_n(\boldsymbol{\omega})] \rightarrow J(\boldsymbol{\omega}), \quad \text{as } n \rightarrow \infty.$$

We impose a smoothness condition on the weight function g involved in $\psi_{\mathbf{h}}$ and $\tilde{\psi}_{\mathbf{h}}$.

Assumption 2 *The Lipschitz function $g : \Pi^2 \rightarrow \mathbb{R}_+$ satisfies*

$$|g(\boldsymbol{\omega}) - g(\omega_1, \tilde{\omega}_2) - g(\tilde{\omega}_1, \omega_2) + g(\tilde{\boldsymbol{\omega}})| \leq c|\omega_1 - \tilde{\omega}_1||\omega_2 - \tilde{\omega}_2| \quad (7)$$

for all $\boldsymbol{\omega} = (\omega_1, \omega_2)$, $\tilde{\boldsymbol{\omega}} = (\tilde{\omega}_1, \tilde{\omega}_2) \in \Pi^2$ and some constant $c > 0$.

In particular, Assumption 2 holds if g is a product of two Lipschitz continuous functions, i.e., $g(\boldsymbol{\omega}) = g_1(\omega_1)g_2(\omega_2)$ with $g_1, g_2 : \Pi \rightarrow \mathbb{R}_+$ Lipschitz continuous.

Theorem 2 *Under Assumption 1 and Assumption 2, the following weak convergence results hold in the space $\mathbb{C}(\Pi^2)$ of continuous functions on Π^2 ,*

$$\frac{n}{\sqrt{m_n}}(\tilde{J}_n - \mathbb{E}[\tilde{J}_n]) \xrightarrow{d} G. \quad (8)$$

Here, the limiting field G is given by $G = \sum_{\mathbf{h} \in \mathbb{Z}^2} \psi_{\mathbf{h}} Z_{\mathbf{h}}$, where $(Z_{\mathbf{h}})$ is a mean-zero Gaussian random field with the covariance function $\text{cov}(Z_{\mathbf{h}_1}, Z_{\mathbf{h}_2})$ detailed in Appendix B.2 of the Supplementary Material (Niu et al., 2025b).

Theorem 2 reveals that the extremal integrated periodogram \tilde{J}_n converges weakly to a Gaussian random field G . An application of the continuous mapping theorem yields the limiting distributions

$$T_n \xrightarrow{d} \sup_{\boldsymbol{\omega} \in \Pi^2} |G(\boldsymbol{\omega})|. \quad (9)$$

4. The bootstrap procedure

4.1. The stationary bootstrap algorithm for random fields

We will develop a bootstrap algorithm for a random field $(X_{\mathbf{t}})_{\mathbf{t} \in \mathbb{Z}^2}$ that is observed on the lattice Λ_n^2 . Suppose that the dependence between $X_{\mathbf{t}}$ and $X_{\mathbf{s}}$ with $\mathbf{t} = (t_1, t_2)$ and $\mathbf{s} = (s_1, s_2)$ depends solely on the horizontal difference $t_1 - s_1$ and the vertical difference $t_2 - s_2$. The stationary bootstrap algorithm for strictly stationary time series is developed in Politis and Romano (1994) as a variant of the block bootstrap method, which produces a conditionally strictly stationary time series. To adapt this to the two-dimensional integer lattice setting, we apply it twice to Λ_n^2 along the horizontal and vertical directions.

- (a) **Horizontal bootstrap:** For $i = 1, \dots, n$, define row vectors $Y_i = ((i, 1), \dots, (i, n))$. Generate i.i.d. sequences (H_{1i}) uniformly distributed on $\{1, \dots, n\}$ and (L_{1i}) geometrically distributed with parameter $\theta = \theta_n \rightarrow 0$. Let $N_1 = \inf\{k : \sum_{i=1}^k L_{1i} \geq n\}$. Concatenate blocks $\{Y_{H_{1j}}, \dots, Y_{H_{1j}+L_{1j}-1}\}$ for $j = 1, \dots, N_1$ (with circular extension), and take the first n elements as $(Y_{t^*})_{t=1}^n$.

- (b) **Vertical bootstrap:** For $i = 1, \dots, n$, define column vectors $Y_i^* = ((1^*, i), \dots, (n^*, i))$. Repeat the procedure in (a) with new independent sequences (H_{2i}) and (L_{2i}) to obtain the bootstrapped sample $(Y_{t^*}^*)_{t=1}^n$, which is exactly Λ_n^{2*} .
- (c) **Bootstrapped sample:** The bootstrapped field for $(X_{\mathbf{t}})_{\mathbf{t} \in \Lambda_n^2}$ is $(X_{\mathbf{t}})_{\mathbf{t} \in \Lambda_n^{2*}}$, or equivalently $(X_{\mathbf{t}^*})_{\mathbf{t} \in \Lambda_n^2}$.

Besides a strictly stationary isotropic random field $(X_{\mathbf{t}})$, we can apply the above algorithm to a Gaussian sheet $(W_{\mathbf{t}})_{\mathbf{t} \in \Lambda_n^2}$, whose covariance function $\rho(\mathbf{h})$ is a production of two autocovariance functions, i.e., $\rho(\mathbf{h}) = \gamma_1(h_1)\gamma_2(h_2)$ for autocovariance functions $\gamma_1, \gamma_2 : \mathbb{Z} \rightarrow \mathbb{R}$ of some time series.

4.2. The bootstrapped extremogram and its asymptotic distribution

Recall the extremal indicator function $I_{\mathbf{t}} = \mathbf{1}(|X_{\mathbf{t}}| > a_{m_n})$ and define $I_{\mathbf{t}}(\mathbf{h}) = I_{\mathbf{t}}I_{\mathbf{t}+\mathbf{h}}$ for $\mathbf{t}, \mathbf{h} \in \mathbb{Z}^2$. Here, we adopt the convention that t_i in $\mathbf{t} = (t_1, t_2)$ is taken modulo n if $|t_i| > n$. When $\mathbf{h} = \mathbf{0}$, $I_{\mathbf{t}}(\mathbf{0}) = I_{\mathbf{t}}$. Since $(X_{\mathbf{t}})$ is strictly stationary and isotropic, the random fields $(I_{\mathbf{t}})_{\mathbf{t} \in \Lambda_n^2}$ and $(I_{\mathbf{t}}(\mathbf{h}))_{\mathbf{t} \in \Lambda_n^2}$ are strictly stationary and isotropic for fixed n and fixed $\mathbf{h} \in \mathbb{Z}^2$. Applying the stationary bootstrap algorithm in Section 4.1 to these two fields yields the bootstrapped index set Λ_n^{2*} , and consequently, we obtain the bootstrapped random field $(I_{\mathbf{t}^*}(\mathbf{h}))_{\mathbf{t} \in \Lambda_n^2}$ with $\mathbf{t}^* \in \Lambda_n^{2*}$.

We define the extremogram based on $(I_{\mathbf{t}^*}(\mathbf{h}))$, named the *bootstrapped extremogram*, by

$$\hat{\gamma}^*(\mathbf{h}) = \frac{m_n}{n^2} \sum_{\mathbf{t} \in \Lambda_n^2} I_{\mathbf{t}^*}(\mathbf{h}).$$

Let $\mathbb{P}^*(\cdot) = \mathbb{P}(\cdot \mid (X_{\mathbf{t}}))$ denote the probability measure generated by the bootstrap procedure. The corresponding expectation, variance and covariance are denoted by

\mathbb{E}^* , var^* , and cov^* , respectively. Due to the conditional stationarity, $I_{\mathbf{t}^*}(\mathbf{h}) \stackrel{d}{=} I_{\mathbf{1}^*}(\mathbf{h})$ for all \mathbf{t} ; additionally, $\mathbf{1}^* = (H_{11}, H_{21})$ is uniformly distributed on Λ_n^2 . Hence,

$$\mathbb{E}^*[\hat{\gamma}^*(\mathbf{h})] = \frac{m_n}{n^2} \sum_{\mathbf{t} \in \Lambda_n^2} \mathbb{E}^*[I_{\mathbf{t}^*}(\mathbf{h})] = \frac{m_n}{n^2} \sum_{\mathbf{t} \in \Lambda_n^2} \frac{1}{n^2} \sum_{\mathbf{s} \in \Lambda_n^2} I_{\mathbf{s}}(\mathbf{h}) = m_n C_n(\mathbf{h}),$$

where $C_n(\mathbf{h}) = \frac{1}{n^2} \sum_{\mathbf{t} \in \Lambda_n^2} I_{\mathbf{t}}(\mathbf{h})$. Due to the isotropic property, we have $C_n(\mathbf{h}) = C_n(h_1, -h_2) = C_n(-h_1, h_2) = C_n(-\mathbf{h})$. Without loss of generality, assume \mathbf{h} has non-negative components. The law of total probability yields that

$$\mathbb{E}[C_n(\mathbf{h})] = \frac{\prod_{i=1}^2 (n - h_i)}{n^2} p_n(\mathbf{h}) + \frac{(n - h_1)h_2}{n^2} p_n(h_1, n - h_2) + \frac{h_1 h_2}{n^2} p_n(n - h_1, n - h_2),$$

and thus, $\mathbb{E}[\mathbb{E}^*[\hat{\gamma}^*(\mathbf{h})]] = m_n \mathbb{E}[C_n(\mathbf{h})] = m_n p_n(\mathbf{h}) + o(1) \rightarrow \gamma(\mathbf{h})$ as $n \rightarrow \infty$.

Theorem 3 *Suppose that the conditions of Theorem 2 hold. If the parameter θ satisfies $\theta = \theta_n = r_n/m_n$,*

$$n^2 \theta^3 \rightarrow 0 \quad \text{and} \quad \frac{m_n^{3/2}}{n \theta^4} \sum_{\|\mathbf{h}\| > r_n} \alpha(\|\mathbf{h}\|) \rightarrow 0 \quad \text{as } n \rightarrow \infty, \quad (10)$$

then for any finite set $A \subset \mathbb{Z}^2$,

$$d\left(\frac{n}{\sqrt{m_n}}(\hat{\gamma}^*(\mathbf{i}) - m_n C_n(\mathbf{i}))_{\mathbf{i} \in A}, (Z_{\mathbf{i}})_{\mathbf{i} \in A}\right) \xrightarrow{\mathbb{P}} 0 \quad \text{as } n \rightarrow \infty, \quad (11)$$

where d is any metric describing weak convergence in an Euclidean space, and $(Z_{\mathbf{i}})_{\mathbf{i} \in A} \sim N(0, \Sigma_A)$ with Σ_A as defined in Theorem 1 of Cho et al. (2016).

Theorem 3 presents the pre-asymptotic central limit theorem for the bootstrapped extremogram $\hat{\gamma}^*$. The parameter $\theta = \theta_n$ determines the efficiency

of the stationary bootstrap algorithm. By choosing $m_n = n^\eta$ and $r_n = \lfloor C \log n \rfloor$ for some $\eta \in (2/3, 1)$ and $C > 0$, it is easy to verify that Assumption 1 holds and θ_n satisfies (10).

4.3. The bootstrapped extremal integrated periodogram and its asymptotic property

We provide the definition of the *bootstrapped extremal integrated periodogram*, $\hat{J}_n^*(\omega)$ for $\omega \in \Pi^2$, along with its asymptotic properties. In the classical time series analysis, it is common to study the *smoothed periodogram* that is a consistent estimator for the spectral density; see e.g. Brockwell and Davis (1991) for example. One way to smooth the periodogram is by truncation. Following this idea, we propose the *truncated extremal periodogram* for (X_t) ,

$$\hat{f}(\omega) = \sum_{\|\mathbf{h}\| \leq r_n} \hat{\gamma}(\mathbf{h}) \cos(\mathbf{h}^\top \omega), \quad \omega \in \Pi^2,$$

where $\hat{\gamma}(\mathbf{h}) = (m_n/n^2) \sum_{\mathbf{t} \in \Lambda_n^2} I_{\mathbf{t}}(\mathbf{h})$. The *truncated extremal integrated periodogram* is given by

$$\hat{J}_n(\omega) = \sum_{\|\mathbf{h}\| \leq r_n} \hat{\gamma}(\mathbf{h}) \tilde{\psi}_{\mathbf{h}}(\omega).$$

By replacing $\hat{\gamma}(\mathbf{h})$ in $\hat{J}_n(\omega)$ with its bootstrapped counterpart $\hat{\gamma}^*(\mathbf{h})$, we obtain the *bootstrapped extremal integrated periodogram*

$$\hat{J}_n^*(\omega) = \sum_{\|\mathbf{h}\| \leq r_n} \hat{\gamma}^*(\mathbf{h}) \tilde{\psi}_{\mathbf{h}}(\omega), \quad \omega \in \Pi^2.$$

The following results establish the uniform convergence in probability of the bootstrapped extremal integrated periodogram.

Theorem 4 *Under the conditions of Theorem 3, the following result holds:*

$$\sup_{\boldsymbol{\omega} \in \Pi^2} \left| \mathbb{E}^* \left[\widehat{J}_n^*(\boldsymbol{\omega}) \right] - J(\boldsymbol{\omega}) \right| \xrightarrow{\mathbb{P}} 0.$$

The following functional central limit theorem for \widehat{J}_n^* is necessary in deriving the asymptotic distribution of the bootstrapped test statistic T_n^* .

Theorem 5 *Assume that the conditions of Theorem 3 hold. Then we have*

$$d \left(\frac{n}{\sqrt{m_n}} \left(\widehat{J}_n^* - \mathbb{E}^*[\widehat{J}_n^*] \right), G \right) \xrightarrow{\mathbb{P}} 0,$$

where G is the same as in (8).

The bootstrapped GRS is given by

$$T_n^* = \frac{n}{\sqrt{m_n}} \sup_{\boldsymbol{\omega} \in \Pi^2} \left| \widehat{J}_n^*(\boldsymbol{\omega}) - \mathbb{E}[\widehat{J}_n^*(\boldsymbol{\omega})] \right|. \quad (12)$$

An application of continuous mapping theorem yields that

$$T_n^* \xrightarrow{d} \sup_{\boldsymbol{\omega} \in \Pi^2} |G(\boldsymbol{\omega})|.$$

The right-hand side of the above limit is the same as the right-hand side of (9).

The bootstrap-based testing procedure involves generating bootstrap samples and computing T_n^* . Denote $c_n^*(\alpha)$ as the corresponding critical value for the test at significance level α . This approach avoids the complex derivation of the theoretical null distribution through bootstrap, while inheriting the accurate characterization of extremal dependence in the simulation-based test.

5. Simulation study

5.1. Examples of max-stable random fields

We focus on two max-stable models with unit Fréchet marginals: the *max-moving averages* field and the *Brown-Resnick* field. Both models are widely used for characterizing spatial extreme events, and have been formally proven to satisfy Assumptions 1 in Damek et al. (2023), making them ideal benchmarks for validating our proposed goodness-of-fit tests.

The *max-moving averages* (MMA) field $(X_{\mathbf{t}})_{\mathbf{t} \in \mathbb{Z}^2}$ is given by

$$X_{\mathbf{t}} = \max_{\mathbf{s} \in \mathbb{Z}^2} w(\mathbf{s}) Z_{\mathbf{t}-\mathbf{s}}, \quad \mathbf{t} \in \mathbb{Z}^2, \quad (13)$$

with non-negative weight function $w(\mathbf{s}) = \phi^{|s_1|+|s_2|} \mathbf{1}(|s_1| + |s_2| \leq 5)$ for $\phi > 0$. Its extremogram is $\gamma(\mathbf{h}) = \sum_{\mathbf{s} \in \mathbb{Z}^2} (\omega(\mathbf{s}) \wedge \omega(\mathbf{s} + \mathbf{h})) / (\sum_{\mathbf{s} \in \mathbb{Z}^2} \omega(\mathbf{s}))$. Another random field is the truncated *Brown-Resnick* (BR) field,

$$X_{\mathbf{s}} = \sup_{1 \leq j \leq 1000} \Gamma_j^{-1} \exp\{W_{\mathbf{s}}^{(j)} - \delta(\mathbf{s})\}, \quad \mathbf{s} \in \Lambda_n^2, \quad (14)$$

where $\Gamma_j = \sum_{i=1}^j E_i$, $j \geq 1$, (E_i) is a sequence of i.i.d. standard exponential random variables, which are independent of the sequence of i.i.d. fractional Brownian sheets $(W_{\mathbf{s}}^{(j)})_{\mathbf{s} \in \Lambda_n^2}$ with the Hurst index $H \in (0, 1)$, and $\delta(\mathbf{s}) = \text{var}(W_{\mathbf{s}}^{(j)})/2$. Its extremogram is $\gamma(\mathbf{h}) = 2(1 - \Psi(\sqrt{\delta(\mathbf{h})}))$, where Ψ denotes the standard normal distribution function. Please refer to Figure 1 for sample paths of (13) and (14).

5.2. Densities of GRS statistics

We compare the null distributions of the simulation-based statistic T_n and bootstrap-based statistic T_n^* for different random fields $(X_{\mathbf{t}})_{\mathbf{t} \in \mathbb{Z}^2}$ and distinct thresholds a_{m_n} .

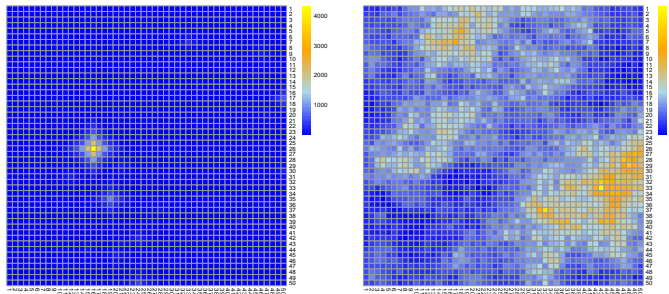


Fig. 1: **Left:** A sample path of the MMA field (13) with $\phi = 0.5$. **Right:** A sample path of the truncated BR field (14) with $H = 0.5$.

By Theorem 2 and Theorem 5, their asymptotic distributions are identical. We simulate these distributions by generating 2,000 replicates via the Monte Carlo method and the bootstrap method. Set the grid size $n = 50$, weight function $g \equiv 1$, and the geometric parameter $\theta = 1/50$ for the stationary bootstrap algorithm. Recall that a_{m_n} is the threshold satisfying $p_n(\mathbf{0}) = \mathbb{P}(|X_{\mathbf{0}}| > a_{m_n}) = m_n^{-1}$ under H_0 . Since our test statistics focus on extremal dependence with a unified threshold, we standardize all fields to have unit Fréchet marginals using the method in Oesting and Strokorb (2022).

Figure 2 and Figure 3 plot the densities of T_n and T_n^* for the MMA and the truncated BR fields, respectively. For the MMA field (13), the densities are insensitive to a_{m_n} but highly sensitive to ϕ , with $\phi = 0.5$ differing in shape from $\phi = 1.0$ and $\phi = 1.5$, which is determined by the inherent properties of the MMA field. For the truncated BR field (14), the density shapes are not sensitive to H and a_{m_n} . In both cases, the densities of the two statistics align closely, confirming the validity of the stationary bootstrap and the use of bootstrapped quantiles $c_n^*(\alpha)$ as critical values in the test.

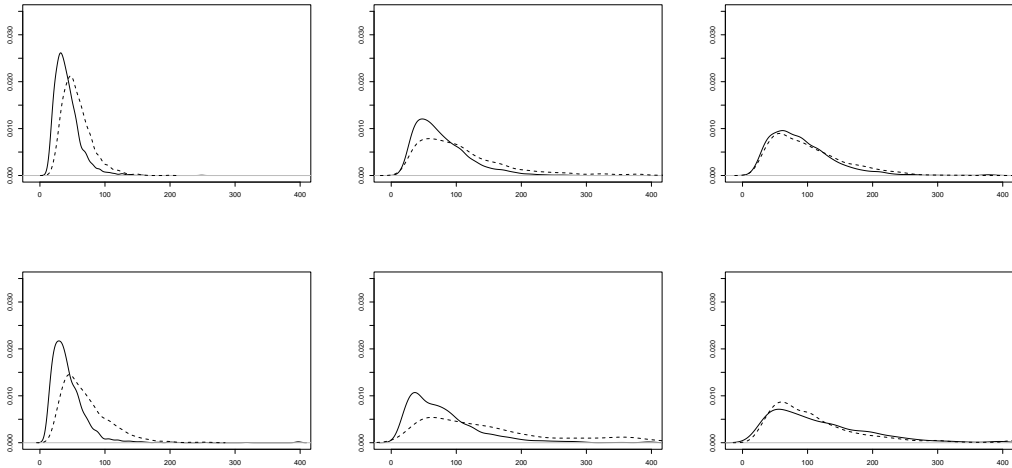


Fig. 2: Densities of the statistics T_n (solid line) and T_n^* (dashed line). The samples are drawn from the MMA fields with $\phi = 0.5, 1.0, 1.5$ in the first, second and third column, and $p_n(\mathbf{0}) = 0.10, 0.05$ in the first and second row, respectively.

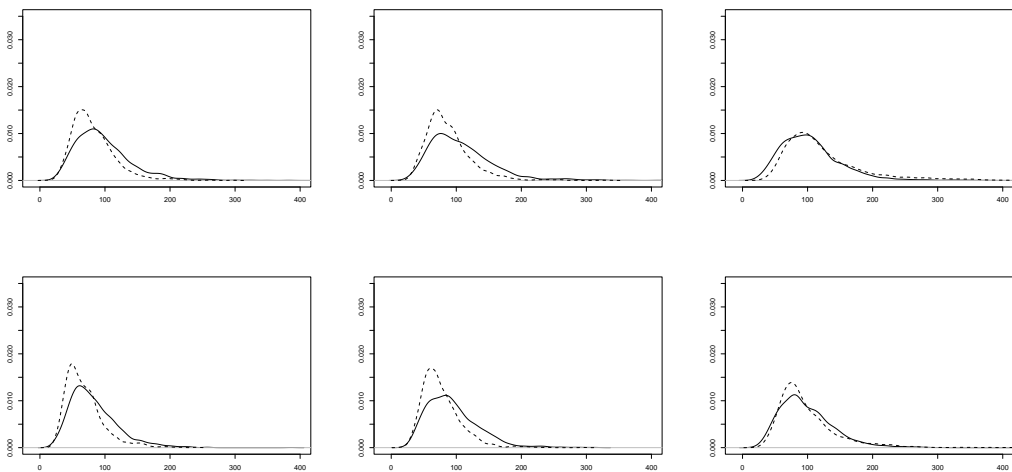


Fig. 3: Densities of the statistics T_n (solid line) and T_n^* (dashed line). The samples are drawn from the BR field with $H = 0.4, 0.5, 0.6$ in the first, second, and third columns, and $p_n(\mathbf{0}) = 0.20, 0.15$ in the first and second rows, respectively.

5.3. Test performances

We present two examples to illustrate the Grenander-Rosenblatt test (GRT) procedure: one uses a simulated MMA field, the other uses a simulated BR field. Each is tested under two null hypotheses: (a) H_0^{MMA} : the observation $(X_{\mathbf{t}})_{\mathbf{t} \in \Lambda_n^2}$ is taken from an MMA field $M_0^{\text{MMA}}(\phi)$; (b) H_0^{BR} : the observation $(X_{\mathbf{t}})_{\mathbf{t} \in \Lambda_n^2}$ is taken from a BR field $M_0^{\text{BR}}(H)$. We choose $p_n(\mathbf{0}) = 0.05$ under H_0^{MMA} and $p_n(\mathbf{0}) = 0.15$ under H_0^{BR} .

In Figure 4, we consider a simulated MMA field (13) with $\phi = 0.5$, whose surface is shown in Figure 1. Under H_0^{MMA} , the Whittle estimation yields $\hat{\phi} = 0.43$. The observed GRS statistic T_n does not exceed either the simulation-based or bootstrap-based critical values (detailed in the left panel of Figure 4), thus we cannot reject H_0^{MMA} . Under H_0^{BR} , the Whittle estimation gives $\hat{H} = 0.40$. The test results differ by different critical values: H_0^{BR} is not rejected via the simulation-based critical value but rejected via the bootstrap-based one; see the right panel of Figure 4.

In Figure 5, we analyze a simulated BR field (14) with $H = 0.5$, whose surface is shown in Figure 1. Under H_0^{MMA} , the Whittle estimation is $\hat{\phi} = 0.23$. The observed T_n exceeds both the simulation-based and bootstrap-based critical values, thus we reject H_0^{MMA} . Under H_0^{BR} , the Whittle estimation gives $\hat{H} = 0.48$. Here, T_n does not exceed either critical value, hence H_0^{BR} is not rejected.

The simulation experiments demonstrate that the GRT performs well in both cases, effectively capturing the characteristics of heavy-tailed random fields. Notably, they highlight the superiority of the test constructed via the stationary bootstrap algorithm. Although the simulation-based and bootstrap-based critical values are asymptotically equivalent, their empirical differences can be substantial. To ensure

the efficiency and reliability of the GRT in practical applications, we thus recommend adopting the minimum of these two candidate critical values.

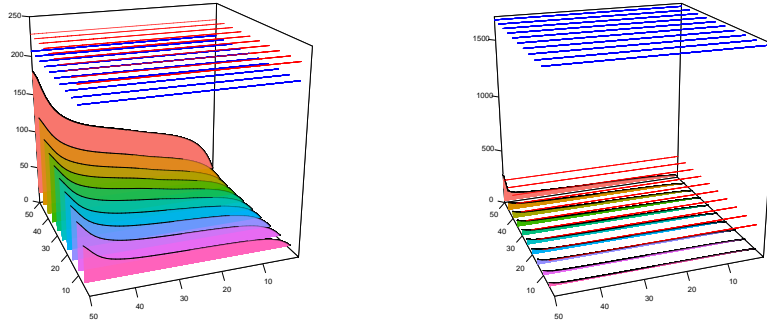


Fig. 4: GRT results for the simulated MMA field with $\phi = 0.5$. **Left:** The surface of the normalized extremal integrated periodogram $\frac{n}{\sqrt{m_n}}|\tilde{J}_n(\omega) - \mathbb{E}[\tilde{J}_n(\omega)]|$ under H_0^{MMA} . Simulation-based critical value (blue line): $c_{50}(0.05) = 206.57$; bootstrap-based critical value (red line): $c_{50}^*(0.05) = 228.19$. **Right:** The same surface under H_0^{BR} . Simulation-based critical value (blue line): $c_{50}(0.05) = 1673.58$; bootstrap-based critical value (red line): $c_{50}^*(0.05) = 218.10$.

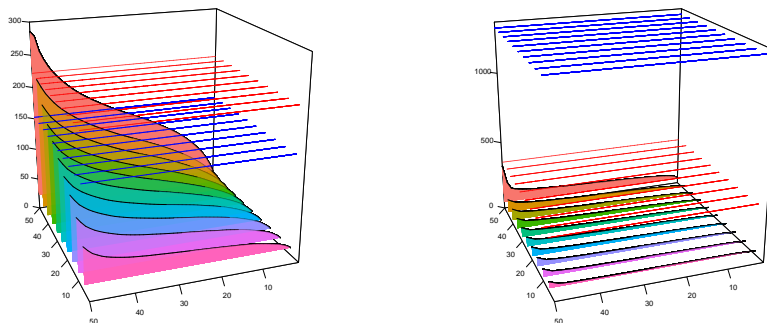


Fig. 5: GRT results for the simulated BR field with $H = 0.5$. **Left:** The surface of the normalized extremal integrated periodogram $\frac{n}{\sqrt{m_n}}|\tilde{J}_n(\omega) - \mathbb{E}[\tilde{J}_n(\omega)]|$ under H_0^{MMA} . Simulation-based critical value (blue line): $c_{50}(0.05) = 152.54$; bootstrap-based critical value (red line): $c_{50}^*(0.05) = 222.29$. **Right:** The same surface under H_0^{BR} . Simulation-based critical value (blue line): $c_{50}(0.05) = 1310.33$; bootstrap-based critical value (red line): $c_{50}^*(0.05) = 353.14$.

6. Real data analysis

6.1. PM2.5 data in Shanghai, China

We consider the Big Data Seamless 1-km Ground-level PM2.5 Dataset for China available on <https://zenodo.org/records/6398971>, which was studied in Wei et al. (2020) and Wei et al. (2021). We focus on the maximum of daily PM2.5 data of 6,402 sampling points in Shanghai from December 18 to December 31, 2021. As shown in Figure 6, we then select the area consisting of 40×40 points (marked red) for the GRT procedure, which covers the central urban district of Shanghai.

Following the methodology in Oesting and Strokorb (2022), we first fit the marginal distribution of the sample with the Generalized Extreme Value (GEV) distribution to estimate the location, scale, and shape parameters, where the location parameter is modeled as a linear function of longitude and latitude. The influence of altitude among points can be ignored due to the flat terrain of Shanghai. Samples drawn from the theoretical model must be transformed into a general max-stable process using the three estimated GEV parameters. To determine a_{m_n} and the simulation-based critical value for the GRT, we simulate the estimated null model 2,000 times. Using the same a_{m_n} , we perform the bootstrap procedure with $\theta = 1/40$ for 2,000 times to obtain the bootstrap-based critical value for the GRT.

Figure 7 displays the normalized extremal integrated periodogram surfaces for PM2.5 data under H_0^{MMA} and H_0^{BR} . For H_0^{MMA} , both simulation-based and bootstrap-based critical values lead to rejection, with the latter providing robust evidence against the null model. For H_0^{BR} , the bootstrap-based critical value rejects it, while the simulation-based one does not. Thus, the GRT rules out the MMA field and reveals a nuanced misfit for the BR model, highlighting its relative strength in capturing the observed extremal dependence.

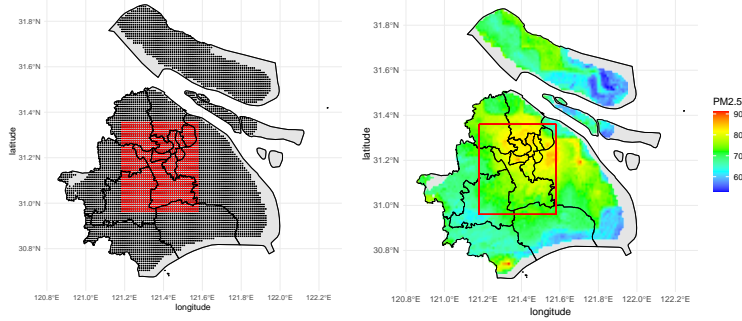


Fig. 6: **Left:** 6402 sampling points at a 1-km resolution (black dots) and the selected 40×40 grid points to be tested (red dots) in Shanghai. **Right:** The maximum of PM2.5 data from December 18 to December 31, 2021 in Shanghai. The red rectangle highlights the area to be tested.

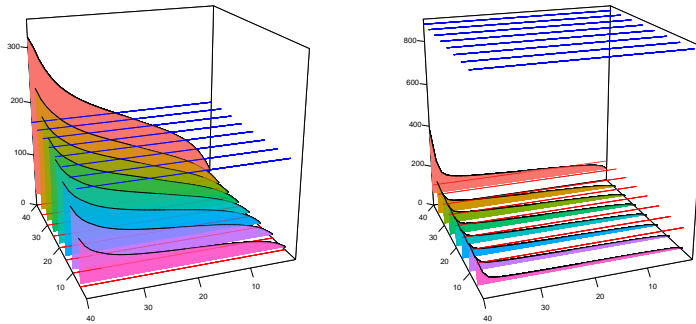


Fig. 7: Surfaces of normalized extremal integrated periodogram for PM2.5 data under two null hypotheses. **Left:** Surface under H_0^{MMA} with the Whittle estimation $\hat{\phi} = 0.22$. Simulation-based critical value (blue line): $c_{40}(0.05) = 162.87$; bootstrap-based critical value (red line): $c_{40}^*(0.05) = 0$. **Right:** Surface under H_0^{BR} with the Whittle estimation $\hat{H} = 0.52$. Simulation-based critical value (blue line): $c_{40}(0.05) = 887.64$; bootstrap-based critical value (red line): $c_{40}^*(0.05) = 104.31$.

6.2. Temperatures in the Netherlands

We further assess our goodness-of-fit test using daily temperature data in the Netherlands, as presented in Oesting and Stokorb (2022). In contrast to the regular and dense data in Section 6.1, this analysis relies on observations from only 18 stations; see the bold black dots in Figure 8. We consider 84 summer days (June 5 –

August 27) from 1990 to 2019 and take the 14-day block maxima of daily temperature at these 18 stations. Focusing on the last block, we interpolate data at 4712 grid points (black dots in Figure 8) via inverse distance weighted interpolation, and then select 35×35 grid points for testing, as shown in Figure 8.

Under H_0^{MMA} , we directly use the interpolated data for Whittle estimation, thereby sampling from the theoretical model. Under H_0^{BR} , we follow the methodology in Oesting and Strokorb (2022) to fit the BR model and to sample from the fitted model at 4,712 grid points by treating these 177 block maxima (30 years with 6 blocks/year, the first three blocks containing missing data) as independent samples with spatial dependence. Here, parameters are estimated using the M-estimator introduced in Einmahl et al. (2016). Given the pairs between stations as in Oesting and Strokorb (2022), we estimate β and s in the variogram of the Brown-Resnick field, $\gamma(\mathbf{h}) = \|\mathbf{h}/s\|^\beta$. The number of samples and the selection of θ in the stationary bootstrap algorithm are the same as in the previous example.

In Figure 9, we plot the surfaces of the extremal integrated periodogram under H_0^{MMA} and H_0^{BR} . It is shown that H_0^{MMA} is not rejected using both simulation-based and bootstrap-based critical values. In contrast, H_0^{BR} is rejected via a bootstrap-based critical value but not a simulation-based one. Unsurprisingly, the distribution of the sample to be tested shows a scattered pattern with some points as extreme values, which aligns sufficiently with the MMA structure.

References

- P. Asadi, A. C. Davison, and S. Engelke. Extremes on river networks. *Ann. Appl. Stat.*, 9(4), 2015.
- B. Basrak and Planinić. Compound poisson approximation for regularly varying fields with application to sequence alignment. *Bernoulli*, 27:1371–1408, 2021.
- B. Basrak and J. Segers. Regularly varying multivariate time series. *Stoch. Proc. Appl.*, 119:1055–1080, 2009.
- P. Billingsley. *Convergence of Probability Measures*. Wiley, New York., 2nd edition, 1999.

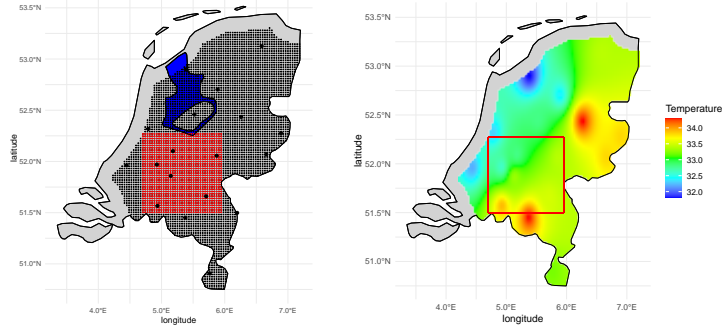


Fig. 8: **Left:** 18 stations (bold black dots), 4,712 inland grid points (black dots), and the selected 35×35 grid points to be tested (red dots) in the Netherlands. **Right:** The interpolated data at these 4,712 inland grid points using the maximum temperature of the 18 stations from August 14 to August 27, 2019. The red rectangle highlights the area to be tested.

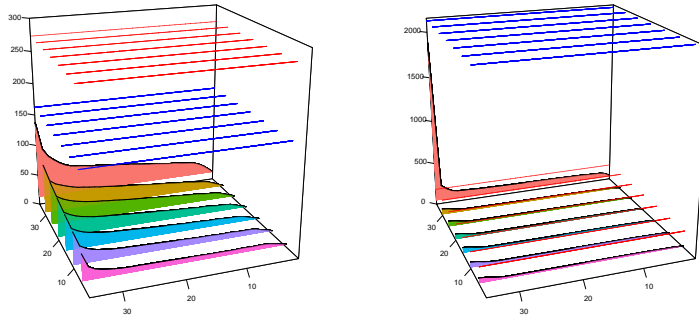


Fig. 9: Surfaces of normalized extremal integrated periodogram for temperature data under two null hypotheses. **Left:** Surface under H_0^{MMA} with the Whittle estimation $\hat{\phi} = 0.39$. Simulation-based critical value (blue line): $c_{35}(0.05) = 162.30$; bootstrap-based critical value (red line): $c_{35}^*(0.05) = 273.31$. **Right:** Surface under H_0^{BR} with parameter estimation $\hat{\beta} = 1.27$ and $\hat{s} = 10.36$ in the variogram $\gamma(\mathbf{h}) = \|\mathbf{h}/s\|^\beta$. Simulation-based critical value (blue line): $c_{35}(0.05) = 2122.75$; bootstrap-based critical value (red line): $c_{35}^*(0.05) = 184.78$.

E. Biswas, A. Kaplan, M. S. Kaiser, and D. J. Nordman. A formal goodness-of-fit test for spatial binary Markov random field models. *Biometrics*, 80(4):ujae119, 2024.

P. Brockwell and R. Davis. *Time Series: Theory and Methods*. Springer, New York, 2nd edition, 1991.

S. Buhl, R. A. Davis, C. Klüppelberg, and C. Steinkohl. Semiparametric estimation for isotropic max-stable space-time processes. *Bernoulli*, 25, 2019.

-
- Y. Cho, R. Davis, and S. Ghosh. Asymptotic properties of the empirical spatial extremogram. *Scand. J. Statist.*, 43:757–773, 2016.
- E. Damek, T. Mikosch, Y. Zhao, and J. Zienkiewicz. Whittle estimation based on the extremal spectral density of a heavy-tailed random field. *Stoc. Proc. Appl.*, 155:232–267, 2023.
- R. Davis and T. Mikosch. The extremogram: a correlogram for extreme events. *Bernoulli*, 15:977–1009, 2009.
- R. Davis, T. Mikosch, and Y. Zhao. Measures of serial extremal dependence and their estimation. *Stoch. Proc. Appl.*, 123:2575–2602, 2013a.
- R. A. Davis, C. Klüppelberg, and C. Steinkohl. Max-stable processes for modeling extremes observed in space and time. *J. Korean Stat. Soc.*, 42(3):399–414, 2013b.
- R. A. Davis, C. Klüppelberg, and C. Steinkohl. Statistical inference for max-stable processes in space and time. *J. R. Stat. Soc. B*, 75(5):791–819, 2013c.
- A. C. Davison and M. M. Gholamrezaee. Geostatistics of extremes. *P. R. Soc. A-Math. Phys.*, 468(2138):581–608, 2012.
- J. H. J. Einmahl, A. Kiriliouk, A. Krajina, and J. Segers. An m-estimator of spatial tail dependence. *J. R. Statist. Soc. B*, 78(1):275–298, 2016.
- P. Embrechts, C. Klüppelberg, and T. Mikosch. *Modelling Extremal Events for Insurance and Finance*. Springer, Berlin, 1997.
- R. Huser and A. C. Davison. Space-time modelling of extreme events. *J. R. Statist. Soc. B*, 76(2):439–461, 2014.
- M. S. Kaiser, S. N. Lahiri, and D. J. Nordman. Goodness of fit tests for a class of markov random field models. *Ann. Stat.*, 40(1), 2012.
- T. Mikosch and Y. Zhao. A fourier analysis of extreme events. *Bernoulli*, 20:803–845, 2014.
- T. Mikosch and Y. Zhao. The integrated periodogram of a dependent extremal event sequence. *Stoch. Proc. Appl.*, 125:3126–3169, 2015.
- W. L. Ng, C. Y. Yau, and X. Chen. Frequency domain bootstrap methods for random fields. *Electron. J. Statist.*, 15(2), 2021.
- Y. Niu, Z. Chen, C. D. Wang, and Y. Zhao. Goodness-of-fit tests for heavy-tailed random fields. 2025a.
- Y. Niu, Z. Chen, C. D. Wang, and Y. Zhao. Supplementary material to “goodness-of-fit tests for heavy-tailed random fields”. 2025b.
- M. Oesting and K. Strokorb. A comparative tour through the simulation algorithms for max-stable processes. *Stat. Sci.*, 37(1):42–63, 2022.
- D. Politis and J. Romano. The stationary bootstrap. *J. Am. Statist. Ass.*, 89:1303–1313, 1994. doi: 10.1080/01621459.1994.10476870.
- M. Rosenblatt. A central limit theorem and a strong mixing condition. *Proc. National Acad. Sci. USA*, 42:43–47, 1956. doi: 10.1073/pnas.42.1.43.
- M. Rosenblatt. *Stationary Sequences and Random Fields*. Birkhauser, Boston, 1985.

-
- J. Segers, Y. Zhao, and T. Meinguet. Polar decomposition of regularly varying time series in star-shaped metric spaces. *Extremes*, 20:539–566, 2017. doi: 10.1007/s10687-017-0287-3.
- J. Wei, Z. Li, M. Cribb, W. Huang, W. Xue, L. Sun, J. Guo, Y. Peng, J. Li, A. Lyapustin, L. Liu, H. Wu, and Y. Song. Improved 1km resolution pm2.5 estimates across china using enhanced space-time extremely randomized trees. *Atmos. Chem. Phys.*, 20(6):3273–3289, 2020.
- J. Wei, Z. Li, A. Lyapustin, L. Sun, Y. Peng, W. Xue, T. Su, and M. Cribb. Reconstructing 1-km-resolution high-quality pm2.5 data records from 2000 to 2018 in china: spatiotemporal variations and policy implications. *Remote. Sens. Environ.*, 252:112136, 2021.
- L. Wu and G. Samorodnitsky. Regularly varying random fields. *Stoch. Proc. Appl.*, 130:4470–4492, 2020.

SUPPLEMENTARY MATERIAL

This supplementary material contains the proofs of the theorems in our main paper (Niu et al., 2025a). Appendix A collects some fundamental results, Appendix B presents the proofs of Theorems 1-2 in Section 3, and Appendix C provides the proofs of Theorems 3-5 in Section 4. Throughout this material, we denote by $c > 0$ a universal constant that may vary across lines.

A. Preliminaries

This section collects some fundamental results that will be used in subsequent proofs.

A.1. Mixing bounds for the extremal indicator processes

The following lemma provides essential bounds for the cross-expectations of the centered extremal indicators $\tilde{I}_{\mathbf{i}}$.

Lemma 1 *Suppose that Assumption 1 is satisfied and let $\mathbf{i}, \mathbf{j}, \mathbf{k}, \mathbf{l} \in \mathbb{Z}^2$. Then the following bounds hold:*

(a) *For $\mathbf{i}, \mathbf{j} \in \mathbb{Z}^2$,*

$$|\mathbb{E}[\tilde{I}_{\mathbf{i}}\tilde{I}_{\mathbf{j}}]| \leq \alpha(\|\mathbf{i} - \mathbf{j}\|).$$

(b) *For $\mathbf{i} \notin \{\mathbf{j}, \mathbf{k}, \mathbf{l}\}$,*

$$|\mathbb{E}[\tilde{I}_{\mathbf{i}}\tilde{I}_{\mathbf{j}}\tilde{I}_{\mathbf{k}}\tilde{I}_{\mathbf{l}}]| \leq c\alpha(d_{\mathbf{i};\mathbf{jkl}}),$$

where $d_{\mathbf{i};\mathbf{jkl}}$ is the distance between $\{\mathbf{i}\}$ and $\{\mathbf{j}, \mathbf{k}, \mathbf{l}\}$ with respect to $\|\cdot\|$.

(c) For disjoint $\{\mathbf{i}, \mathbf{j}\}, \{\mathbf{k}, \mathbf{l}\}$,

$$|\mathbb{E}[\tilde{I}_{\mathbf{i}}\tilde{I}_{\mathbf{j}}\tilde{I}_{\mathbf{k}}\tilde{I}_{\mathbf{l}}] - \mathbb{E}[\tilde{I}_{\mathbf{i}}\tilde{I}_{\mathbf{j}}]\mathbb{E}[\tilde{I}_{\mathbf{k}}\tilde{I}_{\mathbf{l}}]| \leq c\alpha(d_{\mathbf{ij};\mathbf{kl}}),$$

where $d_{\mathbf{ij};\mathbf{kl}}$ is the distance between $\{\mathbf{i}, \mathbf{j}\}$ and $\{\mathbf{k}, \mathbf{l}\}$.

The proof of Lemma 1 is a simple application of Lemma B.1 in Damek et al. (2023) and thus it is omitted.

A.2. Theoretical bounds for second-order differences of the integral kernels

We introduce some notations first. For $\mathbf{h} = (h_1, h_2), \mathbf{j} = (j_1, j_2), \mathbf{j}' = (j'_1, j'_2) \in \mathbb{Z}^2$ and two positive integers q_1 and q_2 , define

$$\begin{aligned}\zeta_{\mathbf{h}}(\boldsymbol{\omega}, \mathbf{j}; g) &= \psi_{\mathbf{h}}(\omega_1 + (j_1 - 1)2^{-2q_1+1}\pi, \omega_2 + (j_2 - 1)2^{-2q_2+1}\pi), \\ \tilde{\zeta}_{\mathbf{h}}(\boldsymbol{\omega}, \mathbf{j}; g) &= \tilde{\psi}_{\mathbf{h}}(\omega_1 + (j_1 - 1)2^{-2q_1+1}\pi, \omega_2 + (j_2 - 1)2^{-2q_2+1}\pi),\end{aligned}$$

and

$$\begin{aligned}\delta_{\mathbf{h}}(\boldsymbol{\omega}, \mathbf{j}, \mathbf{j}') &= \left(\zeta_{\mathbf{h}}(\boldsymbol{\omega}, \mathbf{j}; g) - \zeta_{\mathbf{h}}(\boldsymbol{\omega}, \mathbf{j}', j_2; g) \right) - \left(\zeta_{\mathbf{h}}(\boldsymbol{\omega}, j_1, j'_2; g) - \zeta_{\mathbf{h}}(\boldsymbol{\omega}, \mathbf{j}'; g) \right), \\ \tilde{\delta}_{\mathbf{h}}(\boldsymbol{\omega}, \mathbf{j}, \mathbf{j}') &= \left(\tilde{\zeta}_{\mathbf{h}}(\boldsymbol{\omega}, \mathbf{j}; g) - \tilde{\zeta}_{\mathbf{h}}(\boldsymbol{\omega}, \mathbf{j}', j_2; g) \right) - \left(\tilde{\zeta}_{\mathbf{h}}(\boldsymbol{\omega}, j_1, j'_2; g) - \tilde{\zeta}_{\mathbf{h}}(\boldsymbol{\omega}, \mathbf{j}'; g) \right),\end{aligned}$$

then define

$$\begin{aligned}d_{\mathbf{h}}(\boldsymbol{\omega}, \boldsymbol{\omega}', \mathbf{j}, \mathbf{j}') &= \left(\delta_{\mathbf{h}}(\boldsymbol{\omega}, \mathbf{j}, \mathbf{j}') - \delta_{\mathbf{h}}(\omega'_1, \omega_2, \mathbf{j}, \mathbf{j}') \right) - \left(\delta_{\mathbf{h}}(\omega_1, \omega'_2, \mathbf{j}, \mathbf{j}') - \delta_{\mathbf{h}}(\boldsymbol{\omega}', \mathbf{j}, \mathbf{j}') \right), \\ \tilde{d}_{\mathbf{h}}(\boldsymbol{\omega}, \boldsymbol{\omega}', \mathbf{j}, \mathbf{j}') &= \left(\tilde{\delta}_{\mathbf{h}}(\boldsymbol{\omega}, \mathbf{j}, \mathbf{j}') - \tilde{\delta}_{\mathbf{h}}(\omega'_1, \omega_2, \mathbf{j}, \mathbf{j}') \right) - \left(\tilde{\delta}_{\mathbf{h}}(\omega_1, \omega'_2, \mathbf{j}, \mathbf{j}') - \tilde{\delta}_{\mathbf{h}}(\boldsymbol{\omega}', \mathbf{j}, \mathbf{j}') \right).\end{aligned}$$

The following lemma is required in the applications of the maximal inequality.

Lemma 2 *Under Assumption 2, we have*

$$|d_{\mathbf{h}}(\boldsymbol{\omega}, \boldsymbol{\omega}', \mathbf{j}, \mathbf{j}')| \leq c 2^{-2q_1-2q_2} |\omega_1 - \omega'_1| |\omega_2 - \omega'_2| |j_1 - j'_1| |j_2 - j'_2|, \quad (15)$$

$$|\tilde{d}_{\mathbf{h}}(\boldsymbol{\omega}, \boldsymbol{\omega}', \mathbf{j}, \mathbf{j}')| \leq c 2^{-2q_1-2q_2} |\omega_1 - \omega'_1| |\omega_2 - \omega'_2| |j_1 - j'_1| |j_2 - j'_2|. \quad (16)$$

Proof of Lemma 2 According to the definition of $\psi_{\mathbf{h}}$, we have

$$\begin{aligned} & \zeta_{\mathbf{h}}(\boldsymbol{\omega}, \mathbf{j}; g) - \zeta_{\mathbf{h}}(\boldsymbol{\omega}, j'_1, j_2; g) \\ &= \int_{\omega_1 + (j'_1 - 1)2^{-2q_1+1}\pi}^{\omega_1 + (j_1 - 1)2^{-2q_1+1}\pi} \int_0^{\omega_2 + (j_2 - 1)2^{-2q_2+1}\pi} \cos(h_1 x_1 + h_2 x_2) g(x_1, x_2) \, dx_1 \, dx_2 \\ &= \int_{(j'_1 - 1)2^{-2q_1+1}\pi}^{(j_1 - 1)2^{-2q_1+1}\pi} \int_0^{\omega_2 + (j_2 - 1)2^{-2q_2+1}\pi} \cos(h_1(x_1 + \omega_1) + h_2 x_2) g(x_1 + \omega_1, x_2) \, dx_1 \, dx_2, \\ & \zeta_{\mathbf{h}}(\boldsymbol{\omega}, j_1, j'_2; g) - \zeta_{\mathbf{h}}(\boldsymbol{\omega}, \mathbf{j}'; g) \\ &= \int_{(j'_1 - 1)2^{-2q_1+1}\pi}^{(j_1 - 1)2^{-2q_1+1}\pi} \int_0^{\omega_2 + (j'_2 - 1)2^{-2q_2+1}\pi} \cos(h_1(x_1 + \omega_1) + h_2 x_2) g(x_1 + \omega_1, x_2) \, dx_1 \, dx_2, \\ & \delta_{\mathbf{h}}(\boldsymbol{\omega}, \mathbf{j}, \mathbf{j}') \\ &= \int_{(j'_1 - 1)2^{-2q_1+1}\pi}^{(j_1 - 1)2^{-2q_1+1}\pi} \int_{\omega_2 + (j'_2 - 1)2^{-2q_2+1}\pi}^{\omega_2 + (j_2 - 1)2^{-2q_2+1}\pi} \cos(h_1(x_1 + \omega_1) + h_2 x_2) g(x_1 + \omega_1, x_2) \, dx_1 \, dx_2 \\ &= \int_{(j'_1 - 1)2^{-2q_1+1}\pi}^{(j_1 - 1)2^{-2q_1+1}\pi} \int_{(j'_2 - 1)2^{-2q_2+1}\pi}^{(j_2 - 1)2^{-2q_2+1}\pi} \cos(h_1(x_1 + \omega_1) + h_2(x_2 + \omega_2)) g(x_1 + \omega_1, x_2 + \omega_2) \, dx_1 \, dx_2. \end{aligned}$$

Then, we have

$$\begin{aligned}
& d_{\mathbf{h}}(\boldsymbol{\omega}, \boldsymbol{\omega}', \mathbf{j}, \mathbf{j}') \\
&= \int_{(j'_1-1)2^{-2q_1+1}\pi}^{(j_1-1)2^{-2q_1+1}\pi} \int_{(j'_2-1)2^{-2q_2+1}\pi}^{(j_2-1)2^{-2q_2+1}\pi} \left(\cos(h_1(x_1 + \omega_1) + h_2(x_2 + \omega_2)) g(x_1 + \omega_1, x_2 + \omega_2) \right. \\
&\quad - \cos(h_1(x_1 + \omega'_1) + h_2(x_2 + \omega_2)) g(x_1 + \omega'_1, x_2 + \omega_2) \\
&\quad - \cos(h_1(x_1 + \omega_1) + h_2(x_2 + \omega'_2)) g(x_1 + \omega_1, x_2 + \omega'_2) \\
&\quad \left. + \cos(h_1(x_1 + \omega'_1) + h_2(x_2 + \omega'_2)) g(x_1 + \omega'_1, x_2 + \omega'_2) \right) dx_1 dx_2.
\end{aligned}$$

It is enough to prove that for every $(x_1, x_2) \in \Pi^2$,

$$\begin{aligned}
& \left| \cos(h_1(x_1 + \omega_1)) \cos(h_2(x_2 + \omega_2)) g(x_1 + \omega_1, x_2 + \omega_2) \right. \\
&\quad - \cos(h_1(x_1 + \omega'_1)) \cos(h_2(x_2 + \omega_2)) g(x_1 + \omega'_1, x_2 + \omega_2) \\
&\quad - \cos(h_1(x_1 + \omega_1)) \cos(h_2(x_2 + \omega'_2)) g(x_1 + \omega_1, x_2 + \omega'_2) \\
&\quad \left. + \cos(h_1(x_1 + \omega'_1)) \cos(h_2(x_2 + \omega'_2)) g(x_1 + \omega'_1, x_2 + \omega'_2) \right| \\
&\leq c|\omega_1 - \omega'_1||\omega_2 - \omega'_2|, \tag{17}
\end{aligned}$$

$$\begin{aligned}
& \left| \sin(h_1(x_1 + \omega_1)) \sin(h_2(x_2 + \omega_2)) g(x_1 + \omega_1, x_2 + \omega_2) \right. \\
&\quad - \sin(h_1(x_1 + \omega'_1)) \sin(h_2(x_2 + \omega_2)) g(x_1 + \omega'_1, x_2 + \omega_2) \\
&\quad - \sin(h_1(x_1 + \omega_1)) \sin(h_2(x_2 + \omega'_2)) g(x_1 + \omega_1, x_2 + \omega'_2) \\
&\quad \left. + \sin(h_1(x_1 + \omega'_1)) \sin(h_2(x_2 + \omega'_2)) g(x_1 + \omega'_1, x_2 + \omega'_2) \right| \\
&\leq c|\omega_1 - \omega'_1||\omega_2 - \omega'_2|. \tag{18}
\end{aligned}$$

The proofs of the inequalities (17) and (18) are similar and we will only give the proof of (17) here. The left-hand side of (17) can be rewritten as

$$\begin{aligned} & \left| \left(\cos(h_1(x_1 + \omega_1)) - \cos(h_1(x_1 + \omega'_1)) \right) \left(\cos(h_2(x_2 + \omega_2)) - \cos(h_2(x_2 + \omega'_2)) \right) g(\mathbf{x} + \boldsymbol{\omega}) \right. \\ & + \left(\cos(h_1(x_1 + \omega_1)) - \cos(h_1(x_1 + \omega'_1)) \right) \cos(h_2(x_2 + \omega'_2)) \left(g(\mathbf{x} + \boldsymbol{\omega}) - g(x_1 + \omega_1, x_2 + \omega'_2) \right) \\ & - \cos(h_1(x_1 + \omega'_1)) \left(\cos(h_2(x_2 + \omega_2)) - \cos(h_2(x_2 + \omega'_2)) \right) \left(g(\mathbf{x} + \boldsymbol{\omega}') - g(x_1 + \omega_1, x_2 + \omega'_2) \right) \\ & \left. + \cos(h_1(x_1 + \omega'_1)) \cos(h_2(x_2 + \omega_2)) \right. \\ & \left. \left(g(\mathbf{x} + \boldsymbol{\omega}) - g(x_1 + \omega'_1, x_2 + \omega_2) - g(x_1 + \omega_1, x_2 + \omega'_2) + g(\mathbf{x} + \boldsymbol{\omega}') \right) \right|. \end{aligned}$$

It is easy to show that (17) holds under Assumption 2.

Since $\tilde{d}_{\mathbf{h}}(\boldsymbol{\omega}, \boldsymbol{\omega}', \mathbf{j}, \mathbf{j}')$ is a discretized version of $d_{\mathbf{h}}(\boldsymbol{\omega}, \boldsymbol{\omega}', \mathbf{j}, \mathbf{j}')$, (16) holds by following similar arguments for $d_{\mathbf{h}}(\boldsymbol{\omega}, \boldsymbol{\omega}', \mathbf{j}, \mathbf{j}')$ and applying (17) and (18). \square

A.3. Central limit theorem for the spatial extremogram $\tilde{\gamma}$

The central limit theorem for $\tilde{\gamma}$ is provided in Cho et al. (2016), and it is listed below.

Proposition 1 *Suppose that Assumption 1 holds. Then for any finite set $A \subset \mathbb{Z}^2$,*

$$\frac{n}{\sqrt{m_n}} \left(\tilde{\gamma}(\mathbf{h}) - \mathbb{E}[\tilde{\gamma}(\mathbf{h})] \right)_{\mathbf{h} \in A} \xrightarrow{d} (Z_{\mathbf{h}})_{\mathbf{h} \in A} \sim N(\mathbf{0}, \Sigma_A),$$

where the covariance matrix Σ_A is given in Theorem 1 of Cho et al. (2016).

B. Proofs in Section 3
B.1. Proof of Theorem 1

For h such that $0 < h < r_n < n$ and large n , we have

$$\begin{aligned}
 & E[\tilde{J}_n(\boldsymbol{\omega})] - \tilde{J}(\boldsymbol{\omega}) \\
 &= \sum_{\|\mathbf{h}\| \leq h} (\mathbb{E}[\tilde{\gamma}(\mathbf{h})] - \gamma(\mathbf{h})) \tilde{\psi}_{\mathbf{h}}(\boldsymbol{\omega}) + \sum_{\|\mathbf{h}\| > h} \mathbb{E}[\tilde{\gamma}(\mathbf{h})] \tilde{\psi}_{\mathbf{h}}(\boldsymbol{\omega}) - \sum_{\|\mathbf{h}\| > h} \gamma(\mathbf{h}) \psi_{\mathbf{h}}(\boldsymbol{\omega}) \\
 &=: Q_1 + Q_2 + Q_3.
 \end{aligned}$$

Since $\int_{\Pi^2} g^2(\boldsymbol{\omega}) d\boldsymbol{\omega} < +\infty$, we have $\sup_{\mathbf{h}, \boldsymbol{\omega}} |\tilde{\psi}_{\mathbf{h}}(\boldsymbol{\omega})| < +\infty$. According to the fact that $\mathbb{E}[\tilde{\gamma}(\mathbf{h})] = m_n p_n(\mathbf{h}) - 1/m_n$ and $\gamma(\mathbf{h}) = m_n p_n(\mathbf{h})$, we have

$$|Q_1| \leq \sup_{\mathbf{h}, \boldsymbol{\omega}} |\tilde{\psi}_{\mathbf{h}}(\boldsymbol{\omega})| \sum_{\|\mathbf{h}\| \leq h} |\mathbb{E}[\tilde{\gamma}(\mathbf{h})] - \gamma(\mathbf{h})| \leq ch^2/m_n \rightarrow 0, \quad n \rightarrow \infty, h \rightarrow \infty$$

due to $h^2/m_n \leq r_n^2/m_n \leq r_n^4/m_n \rightarrow 0$. The conditions (5) and (6) imply that

$$|Q_2| \leq cm_n \sum_{h < \|\mathbf{h}\| \leq r_n} p_n(\mathbf{h}) + cm_n \sum_{\|\mathbf{h}\| > r_n} \alpha(\|\mathbf{h}\|) \rightarrow 0, \quad n \rightarrow \infty, h \rightarrow \infty.$$

Since $\sum_{\mathbf{h}} |\gamma(\mathbf{h})| < \infty$, we have $Q_3 \rightarrow 0$ as $n \rightarrow \infty$ and $h \rightarrow \infty$. This completes the proof of Theorem 1.

B.2. Proof of Theorem 2

We provide the explicit form of the covariance function of $(Z_{\mathbf{h}})$ in Theorem 2:

$$\begin{aligned}
\text{cov}(Z_{\mathbf{h}_1}, Z_{\mathbf{h}_2}) &= \limsup_{n \rightarrow \infty} m_n \mathbb{P}(\min(|X_{\mathbf{0}}|, |X_{\mathbf{h}_1}|, |X_{\mathbf{h}_2}|) > a_{m_n}) \\
&\quad + m_n \sum_{\mathbf{s}=(s_1, s_2) \neq \mathbf{0}, \min(s_1, s_2) \geq 0} \left(\mathbb{P}(\min(|X_{\mathbf{0}}|, |X_{\mathbf{h}_1}|, |X_{\mathbf{s}}|, |X_{\mathbf{s}+\mathbf{h}_2}|) > a_{m_n}) \right. \\
&\quad + \mathbb{P}(\min(|X_{\mathbf{0}}|, |X_{\mathbf{h}_2}|, |X_{\mathbf{s}}|, |X_{\mathbf{s}+\mathbf{h}_1}|) > a_{m_n}) \\
&\quad + \mathbb{P}(\min(|X_{s_1, 0}|, |X_{(s_1, 0)+\mathbf{h}_1}|, |X_{0, s_2}|, |X_{(0, s_2)+\mathbf{h}_2}|) > a_{m_n}) \\
&\quad \left. + \mathbb{P}(\min(|X_{0, s_2}|, |X_{(0, s_2)+\mathbf{h}_1}|, |X_{s_1, 0}|, |X_{(s_1, 0)+\mathbf{h}_2}|) > a_{m_n}) \right),
\end{aligned}$$

for any $\mathbf{h}_1, \mathbf{h}_2 \in \mathbb{Z}^2$.

To facilitate the proof, we will first prove the result

$$\frac{n}{\sqrt{m_n}}(J_n - \mathbb{E}[J_n]) \xrightarrow{d} G, \quad (19)$$

where $J_n(\boldsymbol{\omega}) = \sum_{\|\mathbf{h}\| < n} \tilde{\gamma}(\mathbf{h}) \psi_{\mathbf{h}}(\boldsymbol{\omega})$ for $\boldsymbol{\omega} \in \Pi^2$, the random field G is the same as in (8).

The proof of Theorem 2 consists of three parts.

Part 1: We establish the finite-dimensional convergence of the random field in (19). For every $k \geq 1$, an application of Proposition 1 with $A = \{\mathbf{h} \in \mathbb{Z}^2 : \|\mathbf{h}\| < k\}$ yields that

$$\frac{n}{\sqrt{m_n}} \left(\sum_{\|\mathbf{h}\| < k} \psi_{\mathbf{h}}(\tilde{\gamma}(\mathbf{h}) - \mathbb{E}[\tilde{\gamma}(\mathbf{h})]) \right) \xrightarrow{d} \sum_{\|\mathbf{h}\| < k} \psi_{\mathbf{h}} Z_{\mathbf{h}},$$

where $(Z_{\mathbf{h}})$ is a mean zero Gaussian random field with covariance structure specified in Theorem 1 of Cho et al. (2016).

Part 2: We verify the following tightness condition to complete the proof of the weak convergence in (8).

Lemma 3 *Assume that the conditions of Theorem 2 hold. Then for any $\varepsilon > 0$,*

$$\lim_{h \rightarrow \infty} \limsup_{n \rightarrow \infty} \mathbb{P} \left(\frac{n}{\sqrt{m_n}} \sup_{\boldsymbol{\omega} \in \Pi^2} \left| \sum_{\|\mathbf{h}\| > h} \psi_{\mathbf{h}}(\boldsymbol{\omega}) (\tilde{\gamma}(\mathbf{h}) - \mathbb{E}[\tilde{\gamma}(\mathbf{h})]) \right| > \varepsilon \right) = 0. \quad (20)$$

Proof of Lemma 3 It is sufficient to prove the following limit

$$\lim_{h \rightarrow \infty} \limsup_{n \rightarrow \infty} \mathbb{P} \left(\frac{n}{\sqrt{m_n}} \sup_{\boldsymbol{\omega} \in \Pi^2} \left| \sum_{h_1=h+1}^{n-1} \sum_{h_2=h+1}^{n-1} \psi_{\mathbf{h}}(\boldsymbol{\omega}) (\tilde{\gamma}(\mathbf{h}) - \mathbb{E}[\tilde{\gamma}(\mathbf{h})]) \right| > 2\varepsilon \right) = 0 \quad (21)$$

holds for $\varepsilon > 0$. Without loss of generality, we assume that $h = 2^a - 1$ and $n = 2^{b+1}$, where a and b satisfying $a < b$ are positive integers. A slight modification of the proof is required when h and n do not have such representations, which is omitted for the ease of the explanation.

Let $\varepsilon_{\mathbf{q}} = 2^{-2(q_1+q_2)/\kappa}$ for $\mathbf{q} = (q_1, q_2)$ with integers $q_1, q_2 > 0$ and some $\kappa > 0$ chosen later. Fix $\varepsilon > 0$. Let

$$\begin{aligned}
Q &= \mathbb{P}\left(\frac{n}{\sqrt{m_n}} \sup_{\boldsymbol{\omega} \in \Pi^2} \left| \sum_{h_1=2^a}^{2^{b+1}-1} \sum_{h_2=2^a}^{2^{b+1}-1} \psi_{\mathbf{h}}(\boldsymbol{\omega}) (\tilde{\gamma}(\mathbf{h}) - \mathbb{E}[\tilde{\gamma}(\mathbf{h})]) \right| > 2\varepsilon\right) \\
&\leq \mathbb{P}\left(\frac{n}{\sqrt{m_n}} \sum_{q_1, q_2=a}^b \sup_{\boldsymbol{\omega} \in \Pi^2} \left| \sum_{h_1=2^{q_1}}^{2^{q_1+1}-1} \sum_{h_2=2^{q_2}}^{2^{q_2+1}-1} \psi_{\mathbf{h}}(\boldsymbol{\omega}) (\tilde{\gamma}(\mathbf{h}) - \mathbb{E}[\tilde{\gamma}(\mathbf{h})]) \right| > 2\varepsilon\right) \\
&\leq \mathbb{P}\left(\sum_{q_1, q_2=a}^b \varepsilon_{\mathbf{q}} > 2\varepsilon\right) \\
&\quad + \mathbb{P}\left(\bigcup_{q_1, q_2=a}^b \left\{ \frac{n}{\sqrt{m_n}} \sup_{\boldsymbol{\omega} \in \Pi^2} \left| \sum_{h_1=2^{q_1}}^{2^{q_1+1}-1} \sum_{h_2=2^{q_2}}^{2^{q_2+1}-1} \psi_{\mathbf{h}}(\boldsymbol{\omega}) (\tilde{\gamma}(\mathbf{h}) - \mathbb{E}[\tilde{\gamma}(\mathbf{h})]) \right| > \varepsilon_{\mathbf{q}} \right\}\right) \\
&\leq \sum_{q_1, q_2=a}^b \mathbb{P}\left(\frac{n}{\sqrt{m_n}} \sup_{\boldsymbol{\omega} \in \Pi^2} \left| \sum_{h_1=2^{q_1}}^{2^{q_1+1}-1} \sum_{h_2=2^{q_2}}^{2^{q_2+1}-1} \psi_{\mathbf{h}}(\boldsymbol{\omega}) (\tilde{\gamma}(\mathbf{h}) - \mathbb{E}[\tilde{\gamma}(\mathbf{h})]) \right| > \varepsilon_{\mathbf{q}}\right) \\
&=: \sum_{q_1, q_2=a}^b Q_{\mathbf{q}}.
\end{aligned}$$

In the above inequalities, we use the fact that the probability $\mathbb{P}(\sum_{q_1, q_2=a}^b \varepsilon_{\mathbf{q}} > \varepsilon) = 0$ when a is large enough.

Given $\mathbf{v} = (v_1, v_2)$ with integers v_1 and v_2 , define $L_{\mathbf{qv}} = \{((v_1 - 1)2^{q_1} + l_1, (v_2 - 1)2^{q_2} + l_2) : 1 \leq l_j \leq 2^{q_j}, j = 1, 2\}$ as a set of vectors of integers. For $\mathbf{j} \in L_{\mathbf{qv}}$ and $\boldsymbol{\omega} \in \prod_{j=1}^2 [0, 2^{-2q_j+1}\pi]$, write

$$\begin{aligned}
Y_{\mathbf{qj}}(\boldsymbol{\omega}) &= \frac{n}{\sqrt{m_n}} \sum_{h_1=2^{q_1}}^{2^{q_1+1}-1} \sum_{h_2=2^{q_2}}^{2^{q_2+1}-1} \psi_{\mathbf{h}}(\omega_1 + (j_1 - 1)2^{-2q_1+1}\pi, \\
&\quad \omega_2 + (j_2 - 1)2^{-2q_2+1}\pi) (\tilde{\gamma}(\mathbf{h}) - \mathbb{E}[\tilde{\gamma}(\mathbf{h})]).
\end{aligned}$$

We have

$$\begin{aligned}
Q_{\mathbf{q}} &= \mathbb{P} \left(\frac{n}{\sqrt{m_n}} \max_{1 \leq v_i \leq 2^{q_i}, i=1,2} \max_{\mathbf{j} \in L_{\mathbf{q}\mathbf{v}}} \sup_{\boldsymbol{\omega} \in \prod_{i=1}^2 [(j_i-1)2^{-2q_i+1}\pi, j_i 2^{-2q_i+1}\pi]} \right. \\
&\quad \left. \left| \sum_{h_1=2^{q_1}}^{2^{q_1+1}-1} \sum_{h_2=2^{q_2}}^{2^{q_2+1}-1} \psi_{\mathbf{h}}(\boldsymbol{\omega}) (\tilde{\gamma}(\mathbf{h}) - \mathbb{E}[\tilde{\gamma}(\mathbf{h})]) \right| > \varepsilon_{\mathbf{q}} \right) \\
&\leq \sum_{v_1=1}^{2^{q_1}} \sum_{v_2=1}^{2^{q_2}} \mathbb{P} \left(\max_{\mathbf{j} \in L_{\mathbf{q}\mathbf{v}}} \sup_{\boldsymbol{\omega} \in \prod_{i=1}^2 [0, 2^{-2q_i+1}\pi]} |Y_{\mathbf{qj}}(\boldsymbol{\omega})| > \varepsilon_{\mathbf{q}} \right) \\
&=: \sum_{v_1=1}^{2^{q_1}} \sum_{v_2=1}^{2^{q_2}} Q_{\mathbf{q}\mathbf{v}}.
\end{aligned}$$

Recall the definition of $d_{\mathbf{h}}(\boldsymbol{\omega}, \boldsymbol{\omega}', \mathbf{j}, \mathbf{j}')$ above Lemma 2. Our next task is to derive the upper bound of $Q_{\mathbf{q}\mathbf{v}}$, which needs to prove the inequality

$$\begin{aligned}
\frac{n^2}{m_n} \mathbb{E} \left[\sum_{h_1=2^{q_1}}^{2^{q_1+1}-1} \sum_{h_2=2^{q_2}}^{2^{q_2+1}-1} (\tilde{\gamma}(\mathbf{h}) - \mathbb{E}[\tilde{\gamma}(\mathbf{h})]) d_{\mathbf{h}}(\boldsymbol{\omega}, \boldsymbol{\omega}', \mathbf{j}, \mathbf{j}') \right]^2 &\leq c \prod_{i=1}^2 2^{-2q_i} |j_i - j'_i|^2 |\omega_i - \omega'_i|^2 K_{hn}, \\
\end{aligned} \tag{22}$$

where K_{hn} satisfies $\lim_{h \rightarrow \infty} \limsup_{n \rightarrow \infty} K_{hn} = 0$.

According to Lemma 2, we have

$$|d_{\mathbf{h}}(\boldsymbol{\omega}, \boldsymbol{\omega}', \mathbf{j}, \mathbf{j}')| \leq c \prod_{i=1}^2 2^{-2q_i} |j_i - j'_i| |\omega_i - \omega'_i|.$$

Thus,

$$\begin{aligned} & \frac{n^2}{m_n} \mathbb{E} \left[\left(\sum_{h_1=2^{q_1}}^{2^{q_1+1}-1} \sum_{h_2=2^{q_2}}^{2^{q_2+1}-1} (\tilde{\gamma}(\mathbf{h}) - \mathbb{E}[\tilde{\gamma}(\mathbf{h})]) d_{\mathbf{h}}(\boldsymbol{\omega}, \boldsymbol{\omega}', \mathbf{j}, \mathbf{j}') \right)^2 \right] \\ & \leq c \prod_{i=1}^2 2^{-4q_i} |j_i - j'_i|^2 |\omega_i - \omega'_i|^2 \left(\frac{n^2}{m_n} \mathbb{E} \left[\left(\sum_{h_1=2^{q_1}}^{2^{q_1+1}-1} \sum_{h_2=2^{q_2}}^{2^{q_2+1}-1} (\tilde{\gamma}(\mathbf{h}) - \mathbb{E}[\tilde{\gamma}(\mathbf{h})]) \right)^2 \right] \right). \end{aligned}$$

Therefore, it is enough to prove

$$\frac{n^2}{m_n} \mathbb{E} \left[\left(\sum_{h_1=2^{q_1}}^{2^{q_1+1}-1} \sum_{h_2=2^{q_2}}^{2^{q_2+1}-1} (\tilde{\gamma}(\mathbf{h}) - \mathbb{E}[\tilde{\gamma}(\mathbf{h})]) \right)^2 \right] \leq 2^{2q_1+2q_2} K_{hn}. \quad (23)$$

We will consider two cases: (a) $h < \max_{i=1,2} 2^{q_i+1} \leq 3r_n$; (b) $\max_{i=1,2} 2^{q_i+1} > 3r_n$.

Write $\sum_{\mathbf{h}_1, \mathbf{h}_2}^{(\mathbf{q})} = \sum_{h_{11}=2^{q_1}}^{2^{q_1+1}-1} \sum_{h_{12}=2^{q_2}}^{2^{q_2+1}-1} \sum_{h_{21}=2^{q_1}}^{2^{q_1+1}-1} \sum_{h_{22}=2^{q_2}}^{2^{q_2+1}-1}$. Then

$$\begin{aligned} & \frac{n^2}{m_n} \mathbb{E} \left[\left(\sum_{h_1=2^{q_1}}^{2^{q_1+1}-1} \sum_{h_2=2^{q_2}}^{2^{q_2+1}-1} (\tilde{\gamma}(\mathbf{h}) - \mathbb{E}[\tilde{\gamma}(\mathbf{h})]) \right)^2 \right] \\ & = \frac{m_n}{n^2} \sum_{\mathbf{h}_1, \mathbf{h}_2}^{(\mathbf{q})} \sum_{\{(t, \mathbf{s}): \mathbf{t}, \mathbf{t}+\mathbf{h}_1, \mathbf{t}+\mathbf{s}, \mathbf{t}+\mathbf{s}+\mathbf{h}_2 \in \Lambda_n^2\}} (\mathbb{E}[\tilde{I}_{\mathbf{t}} \tilde{I}_{\mathbf{t}+\mathbf{h}_1} \tilde{I}_{\mathbf{t}+\mathbf{s}} \tilde{I}_{\mathbf{t}+\mathbf{s}+\mathbf{h}_2}] - \mathbb{E}[\tilde{I}_{\mathbf{0}} \tilde{I}_{\mathbf{h}_1}] \mathbb{E}[\tilde{I}_{\mathbf{0}} \tilde{I}_{\mathbf{h}_2}]) \\ & \leq m_n \sum_{\mathbf{h}_1, \mathbf{h}_2}^{(\mathbf{q})} \sum_{\mathbf{s}, \mathbf{s}+\mathbf{h}_2 \in \Lambda_n^2} \left| \mathbb{E}[\tilde{I}_{\mathbf{0}} \tilde{I}_{\mathbf{h}_1} \tilde{I}_{\mathbf{s}} \tilde{I}_{\mathbf{s}+\mathbf{h}_2}] - \mathbb{E}[\tilde{I}_{\mathbf{0}} \tilde{I}_{\mathbf{h}_1}] \mathbb{E}[\tilde{I}_{\mathbf{0}} \tilde{I}_{\mathbf{h}_2}] \right| \\ & \leq m_n \sum_{\mathbf{h}_1, \mathbf{h}_2}^{(\mathbf{q})} \left(\sum_{h < \|\mathbf{s}\| \leq r_n} + \sum_{r_n < \|\mathbf{s}\| \leq \|\mathbf{h}_1\| + \|\mathbf{h}_2\| + r_n} + \sum_{\|\mathbf{s}\| > \|\mathbf{h}_1\| + \|\mathbf{h}_2\| + r_n} \right) \\ & \quad \times \left| \mathbb{E}[\tilde{I}_{\mathbf{0}} \tilde{I}_{\mathbf{h}_1} \tilde{I}_{\mathbf{s}} \tilde{I}_{\mathbf{s}+\mathbf{h}_2}] - \mathbb{E}[\tilde{I}_{\mathbf{0}} \tilde{I}_{\mathbf{h}_1}] \mathbb{E}[\tilde{I}_{\mathbf{0}} \tilde{I}_{\mathbf{h}_2}] \right| \\ & = : P_1 + P_2 + P_3. \end{aligned}$$

We assume the first case where $h < \max_{i=1,2} 2^{q_i+1} \leq 3r_n$. We have

$$\begin{aligned}
P_1 &\leq m_n \sum_{\mathbf{h}_1, \mathbf{h}_2}^{(\mathbf{q})} \sum_{h < \|\mathbf{s}\| \leq r_n} (|\mathbb{E}[\tilde{I}_0 \tilde{I}_s \tilde{I}_{\mathbf{h}_1} \tilde{I}_{\mathbf{s}+\mathbf{h}_2}]| + |p_n(\mathbf{h}_1)p_n(\mathbf{h}_2)|) \\
&\leq 2^{2q_1+2q_2} \left(m_n \sum_{h < \|\mathbf{h}\| \leq r_n} p_n(\mathbf{h}) + O(m_n^{-1}) \right), \\
P_2 &\leq m_n \sum_{\mathbf{h}_1, \mathbf{h}_2}^{(\mathbf{q})} \sum_{r_n < \|\mathbf{s}\| \leq \|\mathbf{h}_1\| + \|\mathbf{h}_2\| + r_n} (|\mathbb{E}[\tilde{I}_0 \tilde{I}_s \tilde{I}_{\mathbf{h}_1} \tilde{I}_{\mathbf{s}+\mathbf{h}_2}]| + |p_n(\mathbf{h}_1)p_n(\mathbf{h}_2)|) \\
&\leq 2^{2q_1+2q_2} \left(m_n \sum_{\|\mathbf{h}\| > r_n} \alpha(\|\mathbf{h}\|) + O(m_n^{-1}) \right), \\
P_3 &\leq 2^{2q_1+2q_2} m_n \sum_{\|\mathbf{h}\| > r_n} \alpha(\|\mathbf{h}\|).
\end{aligned}$$

We consider the second case where $\max_{i=1,2} 2^{q_i+1} > 3r_n$. For P_1 ,

$$\begin{aligned}
P_1 &\leq m_n \sum_{\mathbf{h}_1, \mathbf{h}_2}^{(\mathbf{q})} \sum_{h < \|\mathbf{s}\| \leq r_n} (|\mathbb{E}[\tilde{I}_0 \tilde{I}_s \tilde{I}_{\mathbf{h}_1} \tilde{I}_{\mathbf{s}+\mathbf{h}_2}] - \mathbb{E}[\tilde{I}_0 \tilde{I}_s] \mathbb{E}[\tilde{I}_{\mathbf{h}_1} \tilde{I}_{\mathbf{s}+\mathbf{h}_2}]| + |\mathbb{E}[\tilde{I}_0 \tilde{I}_s] \mathbb{E}[\tilde{I}_{\mathbf{h}_1} \tilde{I}_{\mathbf{s}+\mathbf{h}_2}]| \\
&\quad + |\mathbb{E}[\tilde{I}_0 \tilde{I}_{\mathbf{h}_1}] \mathbb{E}[\tilde{I}_0 \tilde{I}_{\mathbf{h}_2}]|) \\
&\leq m_n r_n^2 (\alpha(r_n) + c(p_n(\mathbf{0}))^2 + \alpha(\|\mathbf{h}_1\|)\alpha(\|\mathbf{h}_2\|)) \\
&\leq 2^{2q_1+2q_2} (m_n r_n^2 \alpha(r_n) + O(r_n^2/m_n)).
\end{aligned}$$

For P_2 ,

$$\begin{aligned}
P_2 &\leq m_n \sum_{\mathbf{h}_1, \mathbf{h}_2}^{(\mathbf{q})} \sum_{r_n < \|\mathbf{s}\| \leq \|\mathbf{h}_1\| + \|\mathbf{h}_2\| + r_n} (|\mathbb{E}[\tilde{I}_0 \tilde{I}_s \tilde{I}_{\mathbf{h}_1} \tilde{I}_{\mathbf{s}+\mathbf{h}_2}]| + |\mathbb{E}[\tilde{I}_0 \tilde{I}_{\mathbf{h}_1}] \mathbb{E}[\tilde{I}_0 \tilde{I}_{\mathbf{h}_2}]|) \\
&\leq 2^{2q_1+2q_2} \left(m_n \sum_{\|\mathbf{h}\| > r_n} \alpha(\|\mathbf{h}\|) + m_n n^2 \alpha(\|\mathbf{h}_1\|)\alpha(\|\mathbf{h}_2\|) \right).
\end{aligned}$$

For P_3 ,

$$P_3 \leq 2^{2q_1+2q_2} m_n \sum_{\|\mathbf{h}\| > r_n} \alpha(\|\mathbf{h}\|).$$

Let

$$K_{hn} = m_n \sum_{\|\mathbf{h}\| > r_n} \alpha(\|\mathbf{h}\|) + m_n \sum_{h < \|\mathbf{h}\| \leq r_n} p_n(\mathbf{h}) + cm_n^{-1},$$

which completes the proof of (23).

Notice that

$$\begin{aligned} \mathbb{P}\left(\sup_{\omega \in \prod_{i=1}^2 [0, 2^{-2q_i+1}\pi]} |Y_{\mathbf{qj}} - Y_{\mathbf{qj}'}| > \varepsilon_{\mathbf{q}}\right) &\leq c\varepsilon_{\mathbf{q}}^{-2} \prod_{i=1}^2 2^{-2q_i} (2^{-2q_i+1}\pi)^2 (j_i - j'_i)^2 K_{hn} \\ &\leq c \prod_{i=1}^2 2^{4q_i(\kappa^{-1}-3/2)} (j_i - j'_i)^2 K_{hn}. \end{aligned}$$

In the above inequality, we apply the maximal inequality (Theorem 10.2 in Billingsley (1999)) twice with respect to ω . Now we apply the maximal inequality again to $\sup_{\omega \in \prod_{i=1}^2 [0, 2^{-2q_i+1}\pi]} |Y_{\mathbf{qj}} - Y_{\mathbf{qj}'}|$ with respect to \mathbf{j} and we have

$$Q_{\mathbf{qv}} = \mathbb{P}\left(\max_{\mathbf{j} \in L_{\mathbf{qv}}} \sup_{\omega \in \prod_{i=1}^2 [0, 2^{-2q_i+1}\pi]} |Y_{\mathbf{qj}}| > \varepsilon_{\mathbf{q}}\right) \leq c \prod_{i=1}^2 2^{4q_i(\kappa^{-1}-1/2)} K_{hn}.$$

Thus, we have

$$Q \leq \sum_{q_1, q_2=a}^b \sum_{v_1=1}^{2^{q_1}} \sum_{v_2=1}^{2^{q_2}} Q_{\mathbf{qv}} \leq cK_{hn} \sum_{q_1, q_2=a}^b \prod_{i=1}^2 2^{4q_i(\kappa^{-1}-1/2)}.$$

For $\kappa > 2$, the right-hand side of the above inequality converges to zero by first letting $n \rightarrow \infty$ and then $h \rightarrow \infty$. This completes the proof of Lemma 3. \square

Part 3: We demonstrate that the difference between $J_n(\boldsymbol{\omega}) - \mathbb{E}[J_n(\boldsymbol{\omega})]$ and $\tilde{J}_n(\boldsymbol{\omega}) - \mathbb{E}[\tilde{J}_n(\boldsymbol{\omega})]$ is negligible in probability.

Lemma 4 *Assume that the conditions of Theorem 2 hold. Then for any $\varepsilon > 0$,*

$$\lim_{n \rightarrow \infty} \mathbb{P}\left(\frac{n}{\sqrt{m_n}} \sup_{\boldsymbol{\omega} \in \Pi^2} \left| (J_n(\boldsymbol{\omega}) - \mathbb{E}[J_n(\boldsymbol{\omega})]) - (\tilde{J}_n(\boldsymbol{\omega}) - \mathbb{E}[\tilde{J}_n(\boldsymbol{\omega})]) \right| > \varepsilon\right) = 0.$$

Proof of Lemma 4 For $h \geq 1$, we have

$$\begin{aligned} & \mathbb{P}\left(\frac{n}{\sqrt{m_n}} \sup_{\boldsymbol{\omega} \in \Pi^2} \left| (J_n(\boldsymbol{\omega}) - \mathbb{E}[J_n(\boldsymbol{\omega})]) - (\tilde{J}_n(\boldsymbol{\omega}) - \mathbb{E}[\tilde{J}_n(\boldsymbol{\omega})]) \right| > \varepsilon\right) \\ & \leq \mathbb{P}\left(\frac{n}{\sqrt{m_n}} \sup_{\boldsymbol{\omega} \in \Pi^2} \left| \sum_{\|\mathbf{h}\| \leq h} (\tilde{\gamma}(\mathbf{h}) - \mathbb{E}[\tilde{\gamma}(\mathbf{h})]) (\psi_{\mathbf{h}}(\boldsymbol{\omega}) - \tilde{\psi}_{\mathbf{h}}(\boldsymbol{\omega})) \right| > \varepsilon/3\right) \\ & \quad + \mathbb{P}\left(\frac{n}{\sqrt{m_n}} \sup_{\boldsymbol{\omega} \in \Pi^2} \left| \sum_{\|\mathbf{h}\| > h} (\tilde{\gamma}(\mathbf{h}) - \mathbb{E}[\tilde{\gamma}(\mathbf{h})]) \psi_{\mathbf{h}}(\boldsymbol{\omega}) \right| > \varepsilon/3\right) \\ & \quad + \mathbb{P}\left(\frac{n}{\sqrt{m_n}} \sup_{\boldsymbol{\omega} \in \Pi^2} \left| \sum_{\|\mathbf{h}\| > h} (\tilde{\gamma}(\mathbf{h}) - \mathbb{E}[\tilde{\gamma}(\mathbf{h})]) \tilde{\psi}_{\mathbf{h}}(\boldsymbol{\omega}) \right| > \varepsilon/3\right) \\ & =: V_1 + V_2 + V_3. \end{aligned}$$

According to Lemma 3, we have $V_2 \rightarrow 0$ as $n \rightarrow \infty$. By similar arguments in the proof of Lemma 3, we can show that $V_3 \rightarrow 0$ as $n \rightarrow \infty$ due to Lemma 2. According

to the Cauchy-Schwarz inequality, V_1 has upper bound

$$\begin{aligned}
V_1 &\leq 9\varepsilon^{-2} \frac{n^2}{m_n} \mathbb{E} \left[\sup_{\boldsymbol{\omega} \in \Pi^2} \left| \sum_{\|\mathbf{h}\| \leq h} (\tilde{\gamma}(\mathbf{h}) - \mathbb{E}[\tilde{\gamma}(\mathbf{h})]) (\psi_{\mathbf{h}}(\boldsymbol{\omega}) - \tilde{\psi}_{\mathbf{h}}(\boldsymbol{\omega})) \right|^2 \right] \\
&\leq c \frac{n^2}{m_n} \mathbb{E} \left[\sup_{\boldsymbol{\omega} \in \Pi^2} \sum_{\|\mathbf{h}\| \leq h} (\tilde{\gamma}(\mathbf{h}) - \mathbb{E}[\tilde{\gamma}(\mathbf{h})])^2 \sum_{\|\mathbf{h}\| \leq h} |\psi_{\mathbf{h}}(\boldsymbol{\omega}) - \tilde{\psi}_{\mathbf{h}}(\boldsymbol{\omega})|^2 \right] \\
&\leq ch^2 \frac{n^2}{m_n} \sum_{\|\mathbf{h}\| \leq h} \text{var}(\tilde{\gamma}(\mathbf{h})) \left(\sup_{\|\mathbf{h}\| \leq h, \boldsymbol{\omega} \in \Pi^2} |\psi_{\mathbf{h}}(\boldsymbol{\omega}) - \tilde{\psi}_{\mathbf{h}}(\boldsymbol{\omega})| \right)^2.
\end{aligned}$$

Now we focus on $\sup_{\boldsymbol{\omega} \in \Pi^2} |\psi_{\mathbf{h}}(\boldsymbol{\omega}) - \tilde{\psi}_{\mathbf{h}}(\boldsymbol{\omega})|$. Write $\lambda_j = 2\pi j/n$, $j = 1, \dots, n$ and $x_{in} = \lfloor n\omega_i/2\pi \rfloor$, $i = 1, 2$. Trivially, for $\boldsymbol{\omega} \in \Pi^2$,

$$\begin{aligned}
&\left| \int_{\lambda_{x_{1n}}}^{\omega_1} \int_0^\pi \cos(h_1 x_1 + h_2 x_2) g(x_1, x_2) \, dx_2 \, dx_1 \right| \\
&\quad + \left| \int_{\lambda_{x_{1n}}}^{\omega_1} \int_0^\pi \cos(h_1 x_1 + h_2 x_2) g(x_1, x_2) \, dx_2 \, dx_1 \right| \\
&\quad + \left| \int_{\lambda_{x_{1n}}}^{\omega_1} \int_{\lambda_{x_{2n}}}^{\omega_2} \cos(h_1 x_1 + h_2 x_2) g(x_1, x_2) \, dx_2 \, dx_1 \right| \\
&\leq c/n,
\end{aligned}$$

where c only depends on g . For $\boldsymbol{\omega} \in \Pi^2$,

$$\begin{aligned}
& \left| \psi_{\mathbf{h}}(\lambda_{x_{1n}}, \lambda_{x_{2n}}) - \tilde{\psi}_{\mathbf{h}}(\lambda_{x_{1n}}, \lambda_{x_{2n}}) \right| \\
&= \left| \sum_{i_1=1}^{x_{1n}} \sum_{i_2=1}^{x_{2n}} \int_{\lambda_{i_1-1}}^{\lambda_{i_1}} \int_{\lambda_{i_2-1}}^{\lambda_{i_2}} \left(\cos(h_1 x_1 + h_2 x_2) g(x_1, x_2) - \cos(h_1 \lambda_{i_1} + h_2 \lambda_{i_2}) g(\lambda_{i_1}, \lambda_{i_2}) \right) dx_2 dx_1 \right| \\
&\leq \sum_{i_1=1}^{x_{1n}} \sum_{i_2=1}^{x_{2n}} \int_{\lambda_{i_1-1}}^{\lambda_{i_1}} \int_{\lambda_{i_2-1}}^{\lambda_{i_2}} \left| \cos(h_1 x_1 + h_2 x_2) g(x_1, x_2) - \cos(h_1 x_1 + h_2 x_2) g(\lambda_{i_1}, x_2) \right| \\
&\quad + \left| \cos(h_1 x_1 + h_2 x_2) g(\lambda_{i_1}, x_2) - \cos(h_1 \lambda_{i_1} + h_2 x_2) g(\lambda_{i_1}, x_2) \right| \\
&\quad + \left| \cos(h_1 \lambda_{i_1} + h_2 x_2) g(\lambda_{i_1}, x_2) - \cos(h_1 \lambda_{i_1} + h_2 \lambda_{i_2}) g(\lambda_{i_1}, x_2) \right| \\
&\quad + \left| \cos(h_1 \lambda_{i_1} + h_2 \lambda_{i_2}) g(\lambda_{i_1}, x_2) - \cos(h_1 \lambda_{i_1} + h_2 \lambda_{i_2}) g(\lambda_{i_1}, \lambda_{i_2}) \right| dx_2 dx_1 \\
&\leq ch/n.
\end{aligned}$$

As shown in Proposition 1, $(n^2/m_n) \sum_{\|\mathbf{h}\| \leq h} \text{var}(\tilde{\gamma}(\mathbf{h})) \leq ch^2$. Thus, as $n \rightarrow \infty$,

$$V_1 \leq ch^5/n \rightarrow 0.$$

□

This completes the proof of Theorem 2.

C. Proofs in Section 4

C.1. Proof of Theorem 3

According to the Cramér-Wold device, it is enough to prove that the linear combination with arbitrary coefficients $(a_{\mathbf{i}})_{\mathbf{i} \in A}$,

$$\sum_{\mathbf{i} \in A} a_{\mathbf{i}} (\hat{\gamma}^*(\mathbf{i}) - \mathbb{E}^*[\hat{\gamma}^*(\mathbf{i})])$$

converges in distribution to a normal random variable. For ease of explanation, we assume that the cardinal number of A is 2. Therefore, it is sufficient to prove that for $\mathbf{h}_1, \mathbf{h}_2 \in \mathbb{Z}^2$,

$$\sum_{j=1}^2 a_j (\hat{\gamma}^*(\mathbf{h}_j) - \mathbb{E}^*[\hat{\gamma}^*(\mathbf{h}_j)])$$

converges to a normal random variable. When the cardinal number of A is larger than 2, the arguments are similar.

We introduce the notation. For $\mathbf{t} \in \Lambda_n^2$, write

$$\begin{aligned} I_{\mathbf{t}}(\mathbf{h}) &= I_{\mathbf{t}} I_{\mathbf{t}+\mathbf{h}}, \quad \tilde{I}_{\mathbf{t}}(\mathbf{h}) = I_{\mathbf{t}}(\mathbf{h}) - \mathbb{E}[I_{\mathbf{t}}(\mathbf{h})], \\ I_{\mathbf{t}}(\mathbf{h}_1, \mathbf{h}_2) &= \sum_{j=1}^2 a_j I_{\mathbf{t}}(\mathbf{h}_j), \quad \tilde{I}_{\mathbf{t}}(\mathbf{h}_1, \mathbf{h}_2) = I_{\mathbf{t}}(\mathbf{h}_1, \mathbf{h}_2) - \mathbb{E}[I_{\mathbf{t}}(\mathbf{h}_1, \mathbf{h}_2)], \\ \hat{I}_{\mathbf{t}}(\mathbf{h}) &= I_{\mathbf{t}}(\mathbf{h}) - C_n(\mathbf{h}), \quad \hat{I}_{\mathbf{t}}(\mathbf{h}_1, \mathbf{h}_2) = \sum_{j=1}^2 a_j \hat{I}_{\mathbf{t}}(\mathbf{h}_j). \end{aligned}$$

When $\mathbf{t}, \mathbf{t} + \mathbf{h}, \mathbf{t} + \mathbf{h}_1, \mathbf{t} + \mathbf{h}_2 \in \Lambda_n^2$, $\mathbb{E}[I_{\mathbf{t}}(\mathbf{h})] = p_n(\mathbf{h})$ and $\mathbb{E}[I_{\mathbf{t}}(\mathbf{h}_1, \mathbf{h}_2)] = \sum_{j=1}^2 a_j p_n(\mathbf{h}_j)$. Thus,

$$\begin{aligned} \hat{I}_{\mathbf{t}}(\mathbf{h}) &= \tilde{I}_{\mathbf{t}}(\mathbf{h}) - (C_n(\mathbf{h}) - p_n(\mathbf{h})), \\ \hat{I}_{\mathbf{t}}(\mathbf{h}_1, \mathbf{h}_2) &= \sum_{j=1}^2 a_j (\tilde{I}_{\mathbf{t}}(\mathbf{h}_j) - (C_n(\mathbf{h}_j) - p_n(\mathbf{h}_j))). \end{aligned}$$

The following lemma provides the bound of the difference between $C_n(\mathbf{h})$ and $p_n(\mathbf{h})$.

Lemma 5 *Given the conditions of Theorem 3, the following limit*

$$m_n \mathbb{E}[(C_n(\mathbf{h}) - p_n(\mathbf{h}))^2] = O(r_n^2/n^2), \quad \|\mathbf{h}\| \leq r_n, \quad (24)$$

holds.

Proof of Lemma 5 Since $C_n(\mathbf{h}) - p_n(\mathbf{h}) = n^{-2} \sum_{\mathbf{t} \in \Lambda_n^2} \tilde{I}_{\mathbf{t}}(\mathbf{h})$, we have

$$\begin{aligned} m_n \mathbb{E}[(C_n(\mathbf{h}) - p_n(\mathbf{h}))^2] &\leq \frac{m_n}{n^4} \left(\sum_{\mathbf{t}_1, \mathbf{t}_2 \in \Lambda_n^2, \|\mathbf{t}_1 - \mathbf{t}_2\| \leq r_n} + \sum_{\mathbf{t}_1, \mathbf{t}_2 \in \Lambda_n^2, \|\mathbf{t}_1 - \mathbf{t}_2\| > r_n} \right) \left| \mathbb{E}[\tilde{I}_{\mathbf{t}_1}(\mathbf{h}) \tilde{I}_{\mathbf{t}_2}(\mathbf{h})] \right| \\ &\leq O(r_n^2/n^2) + \frac{m_n}{n^2} \sum_{\|\mathbf{h}\| > r_n} \alpha(\|\mathbf{h}\|). \end{aligned}$$

In the last step, we use the result implied by Lemma B.1 in Damek et al. (2023),

$$\left| \mathbb{E}[\tilde{I}_{\mathbf{t}_1}(\mathbf{h}) \tilde{I}_{\mathbf{t}_2}(\mathbf{h})] \right| \leq c\alpha(\|\mathbf{t}_1 - \mathbf{t}_2\|).$$

Moreover,

$$\frac{n^2}{r_n^2} \left(\frac{m_n}{n^2} \sum_{\|\mathbf{h}\| > r_n} \alpha(\|\mathbf{h}\|) \right) = \frac{1}{r_n^2} m_n \sum_{\|\mathbf{h}\| > r_n} \alpha(\|\mathbf{h}\|) \rightarrow 0, \quad n \rightarrow \infty,$$

and thus we have

$$m_n \mathbb{E}[(C_n(\mathbf{h}) - p_n(\mathbf{h}))^2] = O(r_n^2/n^2).$$

□

To prove (11) in the main paper, it is equivalent to prove the following limit

$$d\left(\frac{n}{\sqrt{m_n}} \sum_{j=1}^2 a_j (\hat{\gamma}^\star(\mathbf{h}_j) - m_n C_n(\mathbf{h}_j)), Z\right) = d\left(\frac{\sqrt{m_n}}{n} \sum_{\mathbf{t} \in \Lambda_n^2} \hat{I}_{\mathbf{t}^\star}(\mathbf{h}_1, \mathbf{h}_2), Z\right) \xrightarrow{\mathbb{P}} 0, \quad (25)$$

where Z is a Gaussian random variable with mean zero.

The proof of (25) consists of two parts.

Part 1: We show that the bootstrapped samples at the locations outside Λ_n^2 are negligible. Write $N_j = \max\{i \geq 1 : \sum_{l=1}^i L_{jl} < n\} + 1$, $j = 1, 2$. Define

$$S_N = \sum_{i_1=1}^{N_1} \sum_{i_2=1}^{N_2} S_n(H_{1i_1}, L_{1i_1}, H_{2i_2}, L_{2i_2}),$$

where

$$S_n(H_{1i_1}, L_{1i_1}, H_{2i_2}, L_{2i_2}) = \frac{m_n}{n^2} \sum_{j=1}^2 \sum_{H_{j,i_j} \leq t_j \leq H_{j,i_j} + L_{j,i_j} - 1} \hat{I}_{\mathbf{t}}(\mathbf{h}_1, \mathbf{h}_2).$$

Lemma 6 *Under the conditions of Theorem 3,*

$$\mathbb{P}^\star\left(\frac{n}{\sqrt{m_n}} \left| \sum_{j=1}^2 a_j (\hat{\gamma}^\star(\mathbf{h}_j) - m_n C_n(\mathbf{h}_j)) - S_N \right| > \delta\right) \xrightarrow{\mathbb{P}} 0, \quad \delta > 0. \quad (26)$$

Proof of Lemma 6 By following the arguments in Politis and Romano (1994), the memoryless property of the geometric distribution and Lemma 5 ensure that

$$\frac{n}{\sqrt{m_n}} \left(\sum_{j=1}^2 a_j (\hat{\gamma}^\star(\mathbf{h}_j) - m_n C_n(\mathbf{h}_j)) - S_N \right)$$

has the distribution

$$\frac{\sqrt{m_n}}{n} \left(\sum_{t_1=H_{11}}^{H_{11}+L_{11}-1} \sum_{t_2=1}^n + \sum_{t_1=1}^n \sum_{t_2=H_{21}}^{H_{21}+L_{21}-1} - \sum_{t_1=H_{11}}^{H_{11}+L_{11}-1} \sum_{t_2=H_{21}}^{H_{21}+L_{21}-1} \right) \hat{I}_{\mathbf{t}}(\mathbf{h}_1, \mathbf{h}_2). \quad (27)$$

We shall prove

$$\frac{\sqrt{m_n}}{n} \sum_{t_1=H_{11}}^{H_{11}+L_{11}-1} \sum_{t_2=1}^n \hat{I}_{\mathbf{t}}(\mathbf{h}_1, \mathbf{h}_2) \xrightarrow{\mathbb{P}} 0,$$

and thus (27) converges in probability to zero by similar arguments. We have

$$\begin{aligned} & \mathbb{E} \left[\mathbb{E}^* \left[\frac{m_n}{n^2} \left(\sum_{t_1=H_{11}}^{H_{11}+L_{11}-1} \sum_{t_2=1}^n \hat{I}_{\mathbf{t}}(\mathbf{h}_1, \mathbf{h}_2) \right)^2 \right] \right] \\ &= \mathbb{E} \left[\mathbb{E} \left[\frac{m_n}{n^2} \left(\sum_{t_1=1}^{L_{11}-1} \sum_{t_2=1}^n \hat{I}_{\mathbf{t}}(\mathbf{h}_1, \mathbf{h}_2) \right)^2 \mid L_{11} \right] \right] \\ &= \sum_{l=1}^{\infty} \theta(1-\theta)^{l-1} \mathbb{E} \left[\frac{m_n}{n^2} \left(\sum_{t_1=1}^{l-1} \sum_{t_2=1}^n \hat{I}_{\mathbf{t}}(\mathbf{h}_1, \mathbf{h}_2) \right)^2 \right] \\ &\leq \sum_{l=1}^{\infty} \theta(1-\theta)^{l-1} \sum_{j=1}^2 2a_j^2 \mathbb{E} \left[\frac{m_n}{n^2} \left(\sum_{t_1=1}^{l-1} \sum_{t_2=1}^n \hat{I}_{\mathbf{t}}(\mathbf{h}_j) \right)^2 \right]. \end{aligned}$$

For fixed l , we can derive an upper bound

$$\begin{aligned}
& \mathbb{E} \left[\frac{m_n}{n^2} \left(\sum_{t_1=1}^{l-1} \sum_{t_2=1}^n \widehat{I}_{\mathbf{t}}(\mathbf{h}_1) \right)^2 \right] \\
&= \frac{m_n}{n^2} \mathbb{E} \left[\sum_{t_{11}=1}^{l-1} \sum_{t_{12}=1}^n \sum_{t_{21}=1}^{l-1} \sum_{t_{22}=1}^n \widehat{I}_{\mathbf{t}_1}(\mathbf{h}_1) \widehat{I}_{\mathbf{t}_2}(\mathbf{h}_1) \right] \\
&\leq \left| \frac{m_n}{n^2} \sum_{t_{11}=1}^{l-1} \sum_{t_{12}=1}^n \sum_{t_{21}=1}^{l-1} \sum_{t_{22}=1}^n \mathbb{E} [\widetilde{I}_{\mathbf{t}_1}(\mathbf{h}_1) \widetilde{I}_{\mathbf{t}_2}(\mathbf{h}_1)] \right| + l^2 m_n \mathbb{E} [(C_n(\mathbf{h}_1) - p_n(\mathbf{h}_1))^2] \\
&=: Q_1 + Q_2.
\end{aligned}$$

According to Assumption 1, we have

$$\begin{aligned}
Q_1 &= \left| \frac{m_n}{n^2} \sum_{t_{11}=1}^{l-1} \sum_{t_{12}=1}^n \left(\sum_{\|\mathbf{t}_2 - \mathbf{t}_1\| \leq h} + \sum_{h < \|\mathbf{t}_2 - \mathbf{t}_1\| \leq r_n} + \sum_{\|\mathbf{t}_2 - \mathbf{t}_1\| > r_n} \right) \mathbb{E} [\widetilde{I}_{\mathbf{t}_1}(\mathbf{h}_1) \widetilde{I}_{\mathbf{t}_2}(\mathbf{h}_1)] \right| \\
&\leq \frac{l}{n} \sum_{\|\mathbf{h}\| \leq h} m_n p_n(\mathbf{h}) + \frac{l}{n} \sum_{h < \|\mathbf{h}\| \leq r_n} m_n p_n(\mathbf{h}) + \frac{l}{n} m_n \sum_{\|\mathbf{h}\| > r_n} \alpha(\|\mathbf{h}\|) + O(l/(nm_n)).
\end{aligned}$$

By Lemma 5, we have $Q_2 \leq cl^2 r_n^2 / n^2$. Therefore, we obtain

$$\begin{aligned}
& \sum_{l=1}^{\infty} \theta(1-\theta)^{l-1} \sum_{j=1}^2 a_j^2 \mathbb{E} \left[\frac{m_n}{n^2} \left(\sum_{t_1=1}^{l-1} \sum_{t_2=1}^n \widehat{I}_{\mathbf{t}}(\mathbf{h}_j) \right)^2 \right] \\
&\leq c \frac{1}{n} \sum_{l=1}^{\infty} l \theta(1-\theta)^{l-1} + c \frac{r_n^2}{n^2} \sum_{l=1}^{\infty} l^2 \theta(1-\theta)^{l-1} \\
&= O((n\theta)^{-1}) + O(r_n^2 (n\theta)^{-2}) \rightarrow 0, \quad n \rightarrow \infty.
\end{aligned}$$

In the last step, we use the condition $m_n/n \rightarrow 0$ and $r_n \rightarrow \infty$. This completes the proof. \square

Part 2: We verify a Lyapunov condition based on Anscombe-type arguments to complete the proof of Theorem 3.

Since $\mathbb{E}^*[S_n(H_{1i_1}, L_{1i_1}, H_{2i_2}, L_{2i_2})] = 0$, we have $\mathbb{E}^*[S_N] = 0$ and the infinite smallest condition conditional on $(X_t)_{t \in \mathbb{Z}^2}$ is satisfied by S_N . By applying a classical Anscombe type argument (see Embrechts et al. (1997), Lemma 2.5.8), the random indices can be replaced by integer sequences $(k_{jn})_{j=1,2;n \in \mathbb{N}}$ such that $k_{jn} \rightarrow \infty$, $n\theta/k_{jn} \rightarrow 1$ as $n \rightarrow \infty$ for $j = 1, 2$. We focus on the asymptotic distribution of

$$\frac{n}{\sqrt{m_n}} \sum_{i_1=1}^{k_{1n}} \sum_{i_2=1}^{k_{2n}} S_n(H_{1i_1}, L_{1i_1}, H_{2i_2}, L_{2i_2}). \quad (28)$$

Note that according to Lemma 5,

$$\begin{aligned} & \frac{n^2}{m_n} k_{1n}^2 k_{2n}^2 \sum_{j=1}^2 a_j^2 m_n^{-1} \left(m_n \mathbb{E}[(C_n(\mathbf{h}_j) - p_n(\mathbf{h}_j))^2] \right) \\ &= O((n^2(n\theta)^4/m_n^2)(r_n^2/n^2)) \\ &= O((n^2\theta^3)^2) \rightarrow 0, \quad n \rightarrow \infty. \end{aligned}$$

In the last step we use (10). Therefore, we can replace $\widehat{I}_t(\mathbf{h}_1, \mathbf{h}_2)$ with $\widetilde{I}_t(\mathbf{h}_1, \mathbf{h}_2)$ in (28) and the asymptotic distribution of (28) remains unchanged.

It is sufficient to prove the limit

$$\frac{\sqrt{m_n}}{n} \sum_{i_1=1}^{k_{1n}} \sum_{i_2=1}^{k_{2n}} \sum_{t_1=H_{1i_1}}^{H_{1i_1}+L_{1i_1}-1} \sum_{t_2=H_{2i_2}}^{H_{2i_2}+L_{2i_2}-1} \widetilde{I}_t(\mathbf{h}_1, \mathbf{h}_2) \xrightarrow{d} Z, \quad (29)$$

where Z is a normal random variable with mean zero. The key step in the proof is the verification of the Lyapunov condition conditional on $(X_{\mathbf{t}})$,

$$\begin{aligned} & \frac{m_n^{3/2}}{n^3} k_{1n} k_{2n} \mathbb{E}^* \left[\left| \sum_{t_1=H_{1i_1}}^{H_{1i_1}+L_{1i_1}-1} \sum_{t_2=H_{2i_2}}^{H_{2i_2}+L_{2i_2}-1} \tilde{I}_{\mathbf{t}}(\mathbf{h}_1, \mathbf{h}_2) \right|^3 \right] \\ & \sim \frac{m_n^{3/2}}{n} \theta^2 \mathbb{E}^* \left[\left| \sum_{t_1=H_{1i_1}}^{H_{1i_1}+L_{1i_1}-1} \sum_{t_2=H_{2i_2}}^{H_{2i_2}+L_{2i_2}-1} \tilde{I}_{\mathbf{t}}(\mathbf{h}_1, \mathbf{h}_2) \right|^3 \right] \\ & \xrightarrow{\mathbb{P}} 0. \end{aligned}$$

Notice that

$$\begin{aligned} & \mathbb{E} \left[\mathbb{E}^* \left[\left| \sum_{t_1=H_{1i_1}}^{H_{1i_1}+L_{1i_1}-1} \sum_{t_2=H_{2i_2}}^{H_{2i_2}+L_{2i_2}-1} \tilde{I}_{\mathbf{t}}(\mathbf{h}_1, \mathbf{h}_2) \right|^3 \right] \right] \\ & = \mathbb{E} \left[\mathbb{E} \left[\left| \sum_{t_1=1}^{L_{1i_1}-1} \sum_{t_2=1}^{L_{2i_2}-1} \tilde{I}_{\mathbf{t}}(\mathbf{h}_1, \mathbf{h}_2) \right|^3 \mid L_{1i_1}, L_{2i_2} \right] \right] \\ & = \sum_{l_1=1}^{\infty} \sum_{l_2=1}^{\infty} (1-\theta)^{l_1+l_2-2} \theta^2 \mathbb{E} \left[\left| \sum_{t_1=1}^{l_1-1} \sum_{t_2=1}^{l_2-1} \tilde{I}_{\mathbf{t}}(\mathbf{h}_1, \mathbf{h}_2) \right|^3 \right]. \end{aligned}$$

For fixed l_1 and l_2 , we have

$$\begin{aligned}
& m_n \mathbb{E} \left[\left| \sum_{t_1=1}^{l_1-1} \sum_{t_2=1}^{l_2-1} \tilde{I}_{\mathbf{t}}(\mathbf{h}_1, \mathbf{h}_2) \right|^3 \right] \\
&= m_n \mathbb{E} \left[\left| \sum_{t_1=1}^{l_1-1} \sum_{t_2=1}^{l_2-1} \tilde{I}_{\mathbf{t}}(\mathbf{h}_1, \mathbf{h}_2) \right| \left(\sum_{t_1=1}^{l_1-1} \sum_{t_2=1}^{l_2-1} \tilde{I}_{\mathbf{t}}(\mathbf{h}_1, \mathbf{h}_2) \right)^2 \right] \\
&\leq m_n \sum_{t_{11}=1}^{l_1-1} \sum_{t_{12}=1}^{l_2-1} \sum_{t_{21}=1}^{l_1-1} \sum_{t_{22}=1}^{l_2-1} \sum_{t_{31}=1}^{l_1-1} \sum_{t_{32}=1}^{l_2-1} \mathbb{E} \left[\left| \tilde{I}_{\mathbf{t}_1}(\mathbf{h}_1, \mathbf{h}_2) \right| \prod_{k=2}^3 \tilde{I}_{\mathbf{t}_k}(\mathbf{h}_1, \mathbf{h}_2) \right] \\
&\leq m_n \left(\sum_{(\mathbf{t}_1, \mathbf{t}_2, \mathbf{t}_3) \in A_1} + \sum_{(\mathbf{t}_1, \mathbf{t}_2, \mathbf{t}_3) \in A_2} + \sum_{(\mathbf{t}_1, \mathbf{t}_2, \mathbf{t}_3) \in A_3} \right) \mathbb{E} \left[\left| \tilde{I}_{\mathbf{t}_1}(\mathbf{h}_1, \mathbf{h}_2) \right| \prod_{k=2}^3 \tilde{I}_{\mathbf{t}_k}(\mathbf{h}_1, \mathbf{h}_2) \right] \\
&=: R_1 + R_2 + R_3,
\end{aligned}$$

where $A_1 = \{(\mathbf{t}_1, \mathbf{t}_2, \mathbf{t}_3) \in \mathbb{N}^6 : 1 \leq t_{ij} \leq l_j - 1, \|\mathbf{t}_k - \mathbf{t}_1\| \leq r_n + \max(\|\mathbf{h}_1\|, \|\mathbf{h}_2\|), i = 1, 2, 3; j = 1, 2; k = 2, 3\}$, $A_2 = \{(\mathbf{t}_1, \mathbf{t}_2, \mathbf{t}_3) \in \mathbb{N}^6 : 1 \leq t_{ij} \leq l_j - 1, \|\mathbf{t}_k - \mathbf{t}_1\| > r_n + \max(\|\mathbf{h}_1\|, \|\mathbf{h}_2\|), \|\mathbf{t}_2 - \mathbf{t}_3\| \leq r_n + \max(\|\mathbf{h}_1\|, \|\mathbf{h}_2\|), i = 1, 2, 3; j = 1, 2; k = 2, 3\}$, and $A_3 = \{(\mathbf{t}_1, \mathbf{t}_2, \mathbf{t}_3) \in \mathbb{N}^6 : 1 \leq t_{ij} \leq l_j - 1, \|\mathbf{t}_k - \mathbf{t}_1\| > r_n + \max(\|\mathbf{h}_1\|, \|\mathbf{h}_2\|), \|\mathbf{t}_2 - \mathbf{t}_3\| > r_n + \max(\|\mathbf{h}_1\|, \|\mathbf{h}_2\|), i = 1, 2, 3; j = 1, 2; k = 2, 3\}$.

We start with R_1 , which has an upper bound

$$|R_1| \leq m_n \sum_{(\mathbf{t}_1, \mathbf{t}_2, \mathbf{t}_3) \in A_1} \left| \mathbb{E} \left[\left| \tilde{I}_{\mathbf{t}_1}(\mathbf{h}_1, \mathbf{h}_2) \right| \prod_{k=2}^3 \tilde{I}_{\mathbf{t}_k}(\mathbf{h}_1, \mathbf{h}_2) \right] \right| \leq cl_1 l_2 r_n^4 m_n p_n(\mathbf{0}).$$

For R_2 , we have

$$\begin{aligned}
|R_2| &\leq m_n \sum_{(\mathbf{t}_1, \mathbf{t}_2, \mathbf{t}_3) \in A_2} \left| \mathbb{E} \left[\left| \tilde{I}_{\mathbf{t}_1}(\mathbf{h}_1, \mathbf{h}_2) \right| \prod_{k=2}^3 \tilde{I}_{\mathbf{t}_k}(\mathbf{h}_1, \mathbf{h}_2) \right] - \mathbb{E} \left[\left| \tilde{I}_{\mathbf{t}_1}(\mathbf{h}_1, \mathbf{h}_2) \right| \right] \mathbb{E} \left[\prod_{k=2}^3 \tilde{I}_{\mathbf{t}_k}(\mathbf{h}_1, \mathbf{h}_2) \right] \right| \\
&\quad + m_n \sum_{(\mathbf{t}_1, \mathbf{t}_2, \mathbf{t}_3) \in A_2} \left| \mathbb{E} \left[\left| \tilde{I}_{\mathbf{t}_1}(\mathbf{h}_1, \mathbf{h}_2) \right| \right] \mathbb{E} \left[\prod_{k=2}^3 \tilde{I}_{\mathbf{t}_k}(\mathbf{h}_1, \mathbf{h}_2) \right] \right| \\
&\leq cl_1 l_2 r_n^2 m_n \sum_{\|\mathbf{h}\| > r_n} \alpha(\|\mathbf{h}\|) + cl_1 l_2 (r_n^2 / m_n) m_n p_n(\mathbf{0}).
\end{aligned}$$

Similarly, we have

$$\begin{aligned}
|R_3| &\leq m_n \sum_{(\mathbf{t}_1, \mathbf{t}_2, \mathbf{t}_3) \in A_3} \left| \mathbb{E} \left[\left| \tilde{I}_{\mathbf{t}_1}(\mathbf{h}_1, \mathbf{h}_2) \right| \prod_{k=2}^3 \tilde{I}_{\mathbf{t}_k}(\mathbf{h}_1, \mathbf{h}_2) \right] - \mathbb{E} \left[\left| \tilde{I}_{\mathbf{t}_1}(\mathbf{h}_1, \mathbf{h}_2) \right| \right] \mathbb{E} \left[\prod_{k=2}^3 \tilde{I}_{\mathbf{t}_k}(\mathbf{h}_1, \mathbf{h}_2) \right] \right| \\
&\quad + m_n \sum_{(\mathbf{t}_1, \mathbf{t}_2, \mathbf{t}_3) \in A_3} \left| \mathbb{E} \left[\left| \tilde{I}_{\mathbf{t}_1}(\mathbf{h}_1, \mathbf{h}_2) \right| \right] \mathbb{E} \left[\prod_{k=2}^3 \tilde{I}_{\mathbf{t}_k}(\mathbf{h}_1, \mathbf{h}_2) \right] \right| \\
&\leq cl_1^3 l_2^3 m_n \sum_{\|\mathbf{h}\| > r_n} \alpha(\|\mathbf{h}\|) + cl_1^3 l_2^3 (m_n p_0) \sum_{\|\mathbf{h}\| > r_n} \alpha(\|\mathbf{h}\|).
\end{aligned}$$

To sum up, we have

$$\begin{aligned}
& \frac{m_n^{3/2}}{n} \theta^2 \mathbb{E} \left[\mathbb{E}^\star \left[\left| \sum_{t_1=H_{1i_1}}^{H_{1i_1}+L_{1i_1}-1} \sum_{t_2=H_{2i_2}}^{H_{2i_2}+L_{2i_2}-1} \tilde{I}_t(\mathbf{h}_1, \mathbf{h}_2) \right|^3 \right] \right] \\
& \leq c \frac{m_n^{1/2} \theta^2}{n} \sum_{l_1=1}^{\infty} \sum_{l_2=1}^{\infty} (1-\theta)^{l_1+l_2-2} \theta^2 \left(l_1 l_2 r_n^4 m_n p_n(\mathbf{0}) + l_1 l_2 (r_n^2/m_n) m_n p_n(\mathbf{0}) \right. \\
& \quad \left. + l_1^3 l_2^3 m_n \sum_{\|\mathbf{h}\| > r_n} \alpha(\|\mathbf{h}\|) \right) \\
& \leq c \frac{m_n^{1/2} r_n^4}{n} + c \frac{m_n^{1/2}}{n \theta^4} m_n \sum_{\|\mathbf{h}\| > r_n} \alpha(\|\mathbf{h}\|) \\
& \rightarrow 0, \quad n \rightarrow \infty.
\end{aligned}$$

This completes the proof of Theorem 3.

□

C.2. Proof of Theorem 4

Since

$$\begin{aligned}
& \left| \mathbb{E}^\star[\hat{J}_n^\star(\omega)] - J(\omega) \right| \\
& \leq \left| \mathbb{E}^\star[\hat{J}_n^\star(\omega)] - \sum_{\|\mathbf{h}\| \leq r_n} m_n p_n(\mathbf{h}) \tilde{\psi}_{\mathbf{h}}(\omega) \right| + \left| \sum_{\|\mathbf{h}\| \leq r_n} m_n p_n(\mathbf{h}) \tilde{\psi}_{\mathbf{h}}(\omega) - \sum_{\|\mathbf{h}\| \leq r_n} m_n p_n(\mathbf{h}) \psi_{\mathbf{h}}(\omega) \right| \\
& \quad + \left| \sum_{\|\mathbf{h}\| \leq r_n} m_n p_n(\mathbf{h}) \psi_{\mathbf{h}}(\omega) - J(\omega) \right|,
\end{aligned}$$

we consider these two parts respectively. For the first part, we have

$$\begin{aligned}
& \mathbb{E} \left[\sup_{\omega \in \Pi^2} \left(\mathbb{E}^\star[\widehat{J}_n^\star(\omega)] - \sum_{\|\mathbf{h}\| \leq r_n} m_n p_n(\mathbf{h}) \psi_{\mathbf{h}}(\omega) \right)^2 \right] \\
&= \mathbb{E} \left[\sup_{\omega \in \Pi^2} m_n^2 \left(\sum_{\|\mathbf{h}\| \leq r_n} (C_n(\mathbf{h}) - p_n(\mathbf{h})) \psi_{\mathbf{h}}(\omega) \right)^2 \right] \\
&= O(m_n r_n^4 / n^2) \\
&= O((r_n^4 / m_n)(m_n^2 / n^2)) \rightarrow 0, \quad n \rightarrow \infty
\end{aligned}$$

by applying Lemma 5. For the second and third parts, we have

$$\begin{aligned}
& \left| \sum_{\|\mathbf{h}\| \leq r_n} m_n p_n(\mathbf{h}) \widetilde{\psi}_{\mathbf{h}}(\omega) - \sum_{\|\mathbf{h}\| \leq r_n} m_n p_n(\mathbf{h}) \psi_{\mathbf{h}}(\omega) \right| \\
& \leq c r_n^2 / n.
\end{aligned}$$

$$\begin{aligned}
& \limsup_{n \rightarrow \infty} \sup_{\omega \in \Pi^2} \left| \sum_{\|\mathbf{h}\| \leq r_n} m_n p_n(\mathbf{h}) \psi_{\mathbf{h}}(\omega) - J(\omega) \right| \\
& \leq c \left(\limsup_{n \rightarrow \infty} \sum_{\|\mathbf{h}\| \leq h} |m_n p_n(\mathbf{h}) - \gamma(\mathbf{h})| + \limsup_{n \rightarrow \infty} \sum_{h < \|\mathbf{h}\| \leq r_n} m_n p_n(\mathbf{h}) + \sum_{\|\mathbf{h}\| > h} \gamma(\mathbf{h}) \right),
\end{aligned}$$

which tends to zero under the conditions of Theorem 4 as $h \rightarrow \infty$.

□

C.3. Proof of Theorem 5

The idea of the proof is similar to Theorem 2. It is enough to show that for some $q_1, q_2 \in \mathbb{N}$ with $2^{\max(q_1, q_2)} < r_n/2$,

$$\frac{n^2}{m_n} \mathbb{E} \left[\left(\sum_{h_1=2^{q_1}}^{2^{q_1+1}-1} \sum_{h_2=2^{q_2}}^{2^{q_2+1}-1} (\hat{\gamma}^*(\mathbf{h}) - \mathbb{E}[\hat{\gamma}^*(\mathbf{h})]) \right)^2 \right] \leq 2^{2q_1+2q_2} K_{hn}, \quad (30)$$

where K_{hn} satisfies $\lim_{h \rightarrow \infty} \limsup_{n \rightarrow \infty} K_{hn} = 0$. The inequality (30) holds if for $h < \|\mathbf{h}_1\|, \|\mathbf{h}_2\| \leq r_n$,

$$\left| \mathbb{E} \left[\frac{n^2}{m_n} \text{cov}^*[\hat{\gamma}^*(\mathbf{h}_1), \hat{\gamma}^*(\mathbf{h}_2)] \right] \right| \leq K_{hn}. \quad (31)$$

Notice that

$$\begin{aligned} & \mathbb{E} \left[\frac{n^2}{m_n} \text{cov}^*[\hat{\gamma}^*(\mathbf{h}_1), \hat{\gamma}^*(\mathbf{h}_2)] \right] \\ &= \frac{m_n}{n^2} \sum_{\mathbf{t} \in \Lambda_n^2} \mathbb{E}[\mathbb{E}^*[\hat{I}_{\mathbf{t}^*}(\mathbf{h}_1) \hat{I}_{\mathbf{t}^*}(\mathbf{h}_2)]] + \frac{m_n}{n^2} \sum_{\mathbf{s} \neq \mathbf{t}} \mathbb{E}[\mathbb{E}^*[\hat{I}_{\mathbf{t}^*}(\mathbf{h}_1) \hat{I}_{\mathbf{s}^*}(\mathbf{h}_2)]] \\ &=: S_1 + S_2. \end{aligned}$$

For S_1 , we have

$$\begin{aligned} \mathbb{E}[S_1] &= \frac{m_n}{n^2} \sum_{\mathbf{t} \in \Lambda_n^2} \mathbb{E}[\hat{I}_{\mathbf{t}}(\mathbf{h}_1) \hat{I}_{\mathbf{t}}(\mathbf{h}_2)] \\ &= \frac{m_n}{n^2} \sum_{\mathbf{t} \in \Lambda_n^2} \mathbb{E}[\tilde{I}_{\mathbf{t}}(\mathbf{h}_1) \tilde{I}_{\mathbf{t}}(\mathbf{h}_2) - \prod_{j=1}^2 (C_n(\mathbf{h}_j) - p_n(\mathbf{h}_j))] \\ &= m_n p_n(\mathbf{0}) + O(r_n^2/n^2). \end{aligned}$$

In the last, we use the result from Lemma 5.

For S_2 , we have

$$\begin{aligned}
S_2 &= \frac{m_n}{n^2} \sum_{\mathbf{t} \in \Lambda_n^2} \sum_{\mathbf{s} \neq \mathbf{0}, \min(s_1, s_2) > 0} \left(\mathbb{E}^*[\widehat{I}_{\mathbf{t}^*}(\mathbf{h}_1) \widehat{I}_{(\mathbf{t}+\mathbf{s})^*}(\mathbf{h}_2)] + \mathbb{E}^*[\widehat{I}_{(\mathbf{t}+\mathbf{s})^*}(\mathbf{h}_1) \widehat{I}_{\mathbf{t}^*}(\mathbf{h}_2)] \right. \\
&\quad \left. + \mathbb{E}^*[\widehat{I}_{(t_1+s_1)^*, (t_2)^*}(\mathbf{h}_1) \widehat{I}_{t_1^*, (t_2+s_2)^*}(\mathbf{h}_2)] + \mathbb{E}^*[\widehat{I}_{(t_1)^*, (t_2+s_2)^*}(\mathbf{h}_1) \widehat{I}_{(t_1+s_1)^*, (t_2)^*}(\mathbf{h}_2)] \right) \\
&=: S_{21} + S_{22} + S_{23} + S_{24}.
\end{aligned}$$

Parts R_{21} and R_{22} have similar structure while S_{23} and S_{24} are similar. We will use S_{21} and S_{23} as examples.

$$\begin{aligned}
&S_{21} \\
&= \frac{m_n}{n^2} \sum_{\mathbf{s} \neq \mathbf{0}, \min(s_1, s_2) \geq 0} \prod_{j=1}^2 (1 - \theta)^{s_j} \sum_{\mathbf{t} \in \Lambda_n^2} (I_{\mathbf{t}}(\mathbf{h}_1) I_{\mathbf{t}+\mathbf{s}}(\mathbf{h}_2) - C_n(\mathbf{h}_1) C_n(\mathbf{h}_2)) \\
&\quad + \frac{m_n}{n^4} \sum_{\mathbf{s} \neq \mathbf{0}, \min(s_1, s_2) \geq 0} \prod_{j=1}^2 (1 - (1 - \theta)^{s_j}) \sum_{\mathbf{t}_1, \mathbf{t}_2 \in \Lambda_n^2} (I_{\mathbf{t}_1}(\mathbf{h}_1) I_{\mathbf{t}_2}(\mathbf{h}_2) - C_n(\mathbf{h}_1) C_n(\mathbf{h}_2)) \\
&\quad + \frac{m_n}{n^3} \sum_{\mathbf{s} \neq \mathbf{0}, \min(s_1, s_2) \geq 0} (1 - (1 - \theta)^{s_1}) (1 - \theta)^{s_2} \sum_{t_1, t_2, t_3=1}^n (I_{\mathbf{t}}(\mathbf{h}_1) I_{t_3, t_2+s_2}(\mathbf{h}_2) - C_n(\mathbf{h}_1) C_n(\mathbf{h}_2)) \\
&\quad + \frac{m_n}{n^3} \sum_{\mathbf{s} \neq \mathbf{0}, \min(s_1, s_2) \geq 0} (1 - \theta)^{s_1} (1 - (1 - \theta)^{s_2}) \sum_{t_1, t_2, t_3=1}^n (I_{\mathbf{t}}(\mathbf{h}_1) I_{t_1+s_1, t_3}(\mathbf{h}_2) - C_n(\mathbf{h}_1) C_n(\mathbf{h}_2)) \\
&=: \sum_{j=1}^4 S_{21j}.
\end{aligned}$$

and

$$\begin{aligned}
& S_{23} \\
&= \frac{m_n}{n^2} \sum_{\mathbf{s} \neq \mathbf{0}, \min(s_1, s_2) \geq 0} \prod_{j=1}^2 (1 - \theta)^{s_j} \sum_{\mathbf{t} \in \Lambda_n^2} (I_{t_1+s_1, t_2}(\mathbf{h}_1) I_{t_1, t_2+s_2}(\mathbf{h}_2) - C_n(\mathbf{h}_1) C_n(\mathbf{h}_2)) \\
&+ \frac{m_n}{n^4} \sum_{\mathbf{s} \neq \mathbf{0}, \min(s_1, s_2) \geq 0} \prod_{j=1}^2 (1 - (1 - \theta)^{s_j}) \sum_{\mathbf{t}_1, \mathbf{t}_2 \in \Lambda_n^2} (I_{\mathbf{t}_1}(\mathbf{h}_1) I_{\mathbf{t}_2}(\mathbf{h}_2) - C_n(\mathbf{h}_1) C_n(\mathbf{h}_2)) \\
&+ \frac{m_n}{n^3} \sum_{\mathbf{s} \neq \mathbf{0}, \min(s_1, s_2) \geq 0} (1 - (1 - \theta)^{s_1}) (1 - \theta)^{s_2} \sum_{t_1, t_2, t_3=1}^n (I_{\mathbf{t}}(\mathbf{h}_1) I_{t_3, t_2+s_2}(\mathbf{h}_2) - C_n(\mathbf{h}_1) C_n(\mathbf{h}_2)) \\
&+ \frac{m_n}{n^3} \sum_{\mathbf{s} \neq \mathbf{0}, \min(s_1, s_2) \geq 0} (1 - \theta)^{s_1} (1 - (1 - \theta)^{s_2}) \sum_{t_1, t_2, t_3=1}^n (I_{t_1+s_1, t_2}(\mathbf{h}_1) I_{t_1, t_3}(\mathbf{h}_2) - C_n(\mathbf{h}_1) C_n(\mathbf{h}_2)) \\
&= : \sum_{j=1}^4 S_{23j}.
\end{aligned}$$

Since

$$\frac{m_n}{n^4} \sum_{\mathbf{t}_1, \mathbf{t}_2 \in \Lambda_n^2} (I_{\mathbf{t}_1}(\mathbf{h}_1) I_{\mathbf{t}_2}(\mathbf{h}_2) - C_n(\mathbf{h}_1) C_n(\mathbf{h}_2)) = 0,$$

we have $S_{212} = S_{232} = 0$.

Parts S_{211} and S_{231} have similar structures while S_{213} , S_{214} , S_{233} and S_{234} are similar. Thus, we will use only S_{211} and S_{233} as examples.

$$\begin{aligned}
\mathbb{E}[S_{211}] &= \frac{m_n}{n^2} \mathbb{E} \left[\sum_{\mathbf{s} \neq \mathbf{0}, \min(s_1, s_2) \geq 0} \prod_{j=1}^2 (1 - \theta)^{s_j} \sum_{\mathbf{t} \in \Lambda_n^2} (\tilde{I}_{\mathbf{t}}(\mathbf{h}_1) \tilde{I}_{\mathbf{t}+\mathbf{s}}(\mathbf{h}_2) - \prod_{j=1}^2 (C_n(\mathbf{h}_j) - p_n(\mathbf{h}_j))) \right] \\
&= \frac{m_n}{n^2} \sum_{0 < \|\mathbf{s}\| < h, \min(s_1, s_2) \geq 0} \prod_{j=1}^2 (1 - \theta)^{s_j} \sum_{\mathbf{t} \in \Lambda_n^2} \mathbb{E} [\tilde{I}_{\mathbf{t}}(\mathbf{h}_1) \tilde{I}_{\mathbf{t}+\mathbf{s}}(\mathbf{h}_2)] + o(1) \\
&= m_n \sum_{0 < \|\mathbf{s}\| < h, \min(s_1, s_2) \geq 0} p_n(\mathbf{s}) + o(1) < \infty.
\end{aligned}$$

In the above equality, we use

$$\left| (m_n n / \theta) \mathbb{E} \left[\prod_{j=1}^2 (C_n(\mathbf{h}_j) - p_n(\mathbf{h}_j)) \right] \right| \rightarrow 0, \quad n \rightarrow \infty,$$

which is implied by Lemma 5.

$$\begin{aligned}
|\mathbb{E}[S_{233}]| &\leq \frac{m_n}{n^3} \left(\sum_{0 \leq s_2 \leq r_n} + \sum_{s_2 > r_n} \right) \sum_{t_2=1}^n \left(\sum_{|t_1-t_3| \leq r_n} + \sum_{|t_1-t_3| > r_n} \right) |\mathbb{E} [\tilde{I}_{\mathbf{t}}(\mathbf{h}_1) \tilde{I}_{t_3, t_2+s_2}(\mathbf{h}_2)]| \\
&\quad + m_n n \sum_{s_2=1}^n (1 - \theta)^{s_2} \left| \mathbb{E} \left[\prod_{j=1}^2 (C_n(\mathbf{h}_j) - p_n(\mathbf{h}_j)) \right] \right| \\
&\leq \frac{m_n}{n^2} \sum_{0 \leq s_2 \leq r_n} \sum_{|t_1-t_3| \leq r_n} |\mathbb{E} [\tilde{I}_{t_1, t_2}(\mathbf{h}_1) \tilde{I}_{t_3, t_2+s_2}(\mathbf{h}_2)]| + c m_n \sum_{\|\mathbf{h}\| > r_n} \alpha(\|\mathbf{h}\|) \\
&\quad + |(m_n n / \theta) \mathbb{E} \left[\prod_{j=1}^2 (C_n(\mathbf{h}_j) - p_n(\mathbf{h}_j)) \right]| \\
&\rightarrow 0, \quad n \rightarrow \infty.
\end{aligned}$$

Therefore, $\lim_{h \rightarrow +\infty} \limsup_{n \rightarrow \infty} K_{hn} = 0$ and this completes the proof of (31).

An auxiliary result from the above calculations is

$$\begin{aligned}
& \limsup_{n \rightarrow \infty} \frac{n^2}{m_n} \mathbb{E} [\text{cov}^*(\hat{\gamma}^*(\mathbf{h}_1), \hat{\gamma}^*(\mathbf{h}_2))] \\
&= \limsup_{n \rightarrow \infty} m_n \mathbb{P}(\min(|X_{\mathbf{0}}|, |X_{\mathbf{h}_1}|, |X_{\mathbf{h}_2}|) > a_{m_n}) \\
&+ m_n \sum_{\min(s_1, s_2) \geq 0, \mathbf{s} \neq \mathbf{0}} \mathbb{P}(\min(|X_{\mathbf{0}}|, |X_{\mathbf{h}_1}|, |X_{\mathbf{s}}|, |X_{\mathbf{s}+\mathbf{h}_2}|) > a_{m_n}) \\
&+ \mathbb{P}(\min(|X_{\mathbf{0}}|, |X_{\mathbf{h}_2}|, |X_{\mathbf{s}}|, |X_{\mathbf{s}+\mathbf{h}_1}|) > a_{m_n}) \\
&+ \mathbb{P}(\min(|X_{s_1,0}|, |X_{(s_1,0)+\mathbf{h}_1}|, |X_{0,s_2}|, |X_{(0,s_2)+\mathbf{h}_2}|) > a_{m_n}) \\
&+ \mathbb{P}(\min(|X_{0,s_2}|, |X_{(0,s_2)+\mathbf{h}_1}|, |X_{s_1,0}|, |X_{(s_1,0)+\mathbf{h}_2}|) > a_{m_n}).
\end{aligned} \tag{32}$$

Now we assume that $h = 2^a - 1$ and $r_n = 2^{b+1}$. Then by following the arguments in the proof of Theorem 2, the proof of Theorem 5 is completed and the details are omitted.

□